Научный совет РАН по физике низкотемпературной плазмы
24 декабря 2020 г.

Диффузные разряды и пучки убегающих электронов, формируемые при высоких напряжениях в неоднородном электрическом поле

Victor F. Tarasenko, D.V. Beloplotov, E.Kh. Baksht,
A.G. Burachenko, И.Д. Костыря, M.I. Lomaev, D.A. Sorokin

High Current Electronics Institute, Tomsk, Russia,

E-mail: VFT@loi.hcei.tsc.ru

Актуальность темы – применения и …

Google Академия

1. Tarasenko, V. (2020). Runaway electrons in diffuse gas discharges. *Plasma Sources Science and Technology*, *29*(3), 034001. (6)
2. Köhn, C., Chanrion, O., Nishikawa, K., Babich, L., & Neubert, T. (2020). The emission of energetic electrons from the complex streamer corona adjacent to leader stepping. *Plasma Sources Science and Technology*, *29*(3), 035023. (6)
3. Lvovskiy, A., Paz-Soldan, C., Eidietis, N. W., Aleynikov, P., Austin, M. E., Dal Molin, A., … & Giacomelli, L. (2020). Runaway electron beam dynamics at low plasma density in DIII-D: energy distribution, current profile, and internal instability. *Nuclear Fusion*, *60*(5), 056008. (5)
4. Mesyats, G. A., Yalandin, M. I., Zubarev, N. M., Sadykova, A. G., Sharypov, K. A., Shpak, V. G., … & Semeniuk, N. S. (2020). How short is the runaway electron flow in an air electrode gap?. *Applied Physics Letters*, *116*(6), 063501. (5)
5. Vallhagen, O., Embreus, O., Pusztai, I., Hesslow, L., & Fülöp, T. (2020). Runaway dynamics in the DT phase of ITER operations in the presence of massive material injection. *Journal of Plasma Physics*, *86*(4). (5)
6. Paz-Soldan, C., Aleynikov, P., Hollmann, E. M., Lvovskiy, A., Bykov, I., Du, X., … & Shiraki, D. (2020). Runaway electron seed formation at reactor-relevant temperature. *Nuclear Fusion*, *60*(5), 056020. (4)

Более 500 публикаций в 2020 году.

Runaway electrons in TOKAMAKs

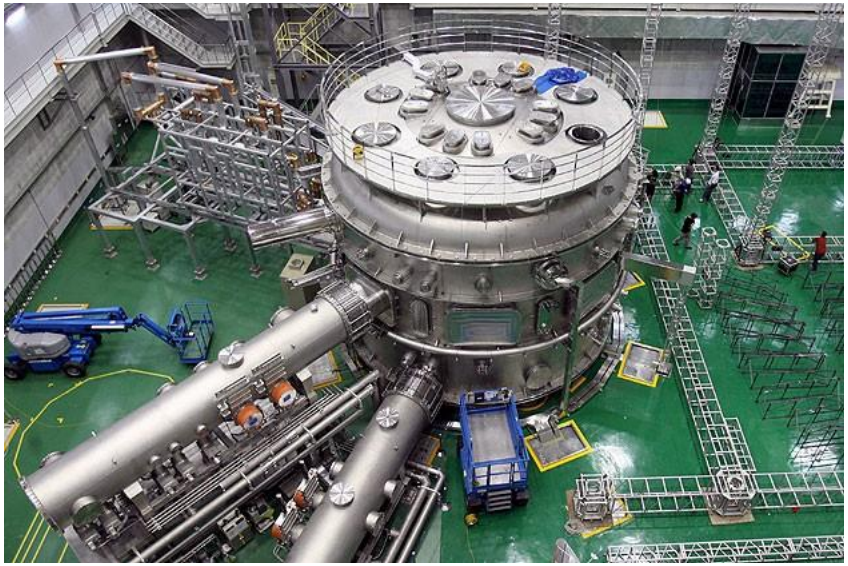

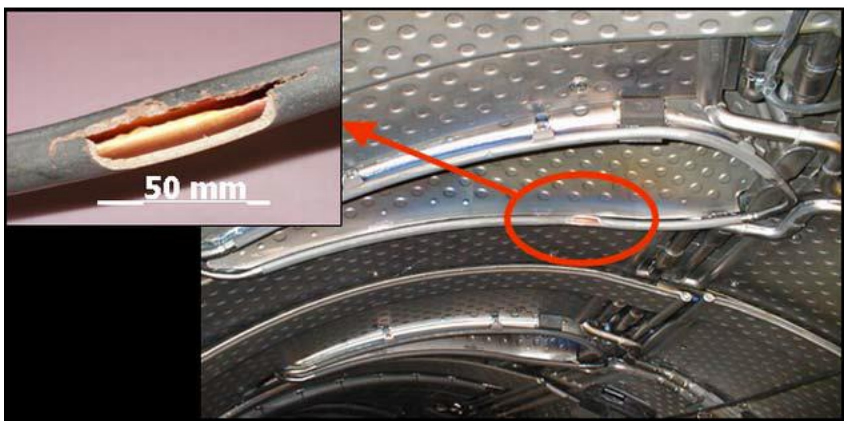

Damage at the edge of the diagnostic port in the vacuum chamber of TORE-SUPRA device, caused by high-energy electron streams.

Runaway electrons in atmospheric discharges

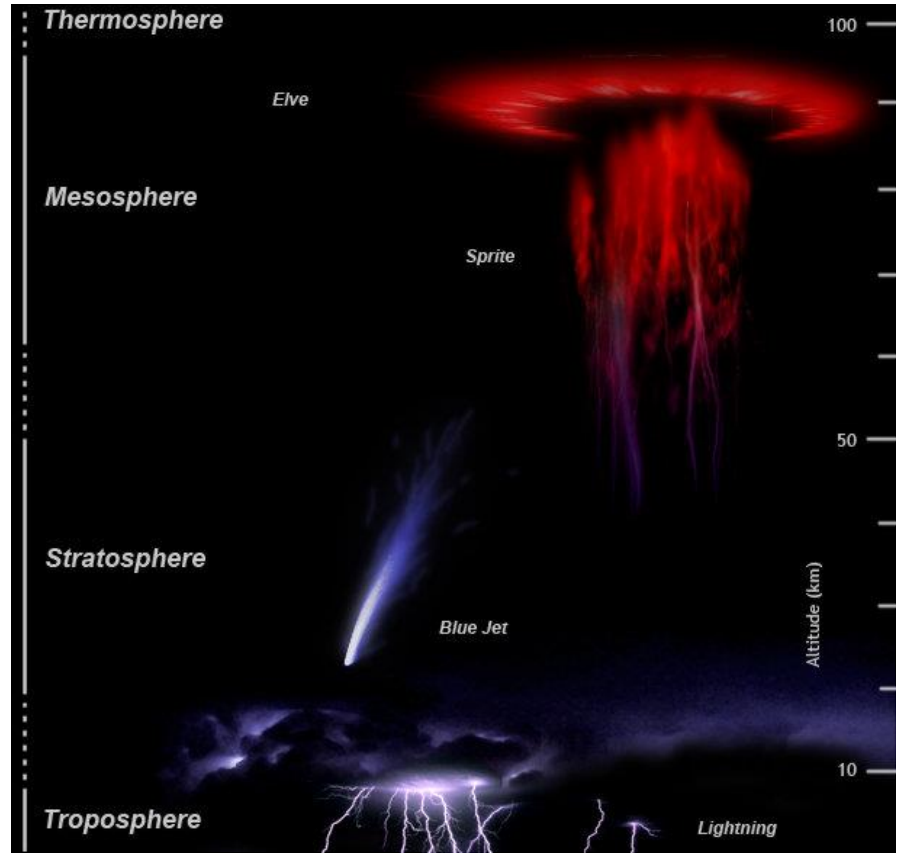

Газовый диод (а), а также диффузный разряд при давлении 1 атмосфера воздуха (б) и азота (в), диаметр трубчатого катода 6 мм, зазор 16 мм.

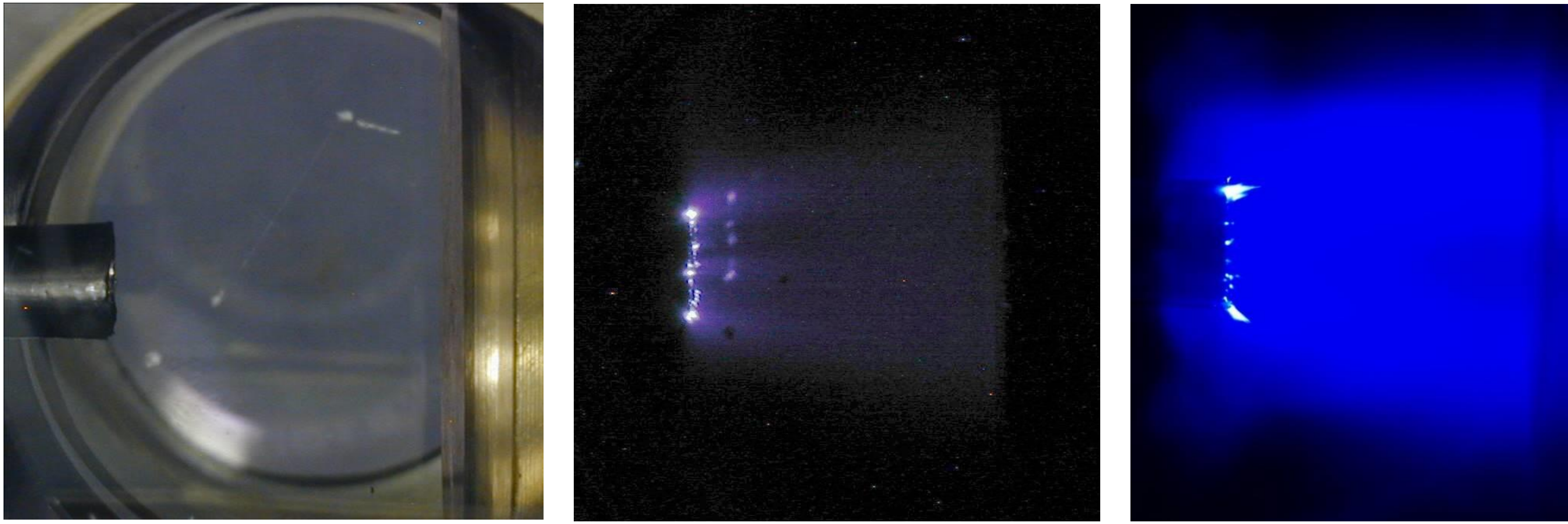

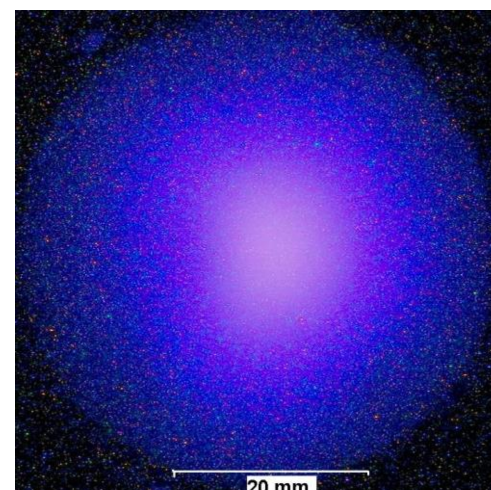

Свечение люминофора под воздействием пучка убегающих электронов

Научный совет РАН по физике низкотемпературной плазмы
24 декабря 2020 г.

План доклада

1. Генерация убегающих электронов (УЭ).
2. Формирование диффузных разрядов (ДР) в результате стримерного пробоя.
3. Переход диффузного разряда в искровую стадию с чёточной структурой
4. Формирование за счёт УЭ импульсов рентгеновского излучения большой длительности.
5. Генерация двух импульсов тока пучка убегающих электронов.
6. Выводы.

Tarasenko V.F. *Review.* (2020). Runaway electrons in diffuse gas discharges. *Plasma Sources Science and Technology*, *29*(3), 034001.

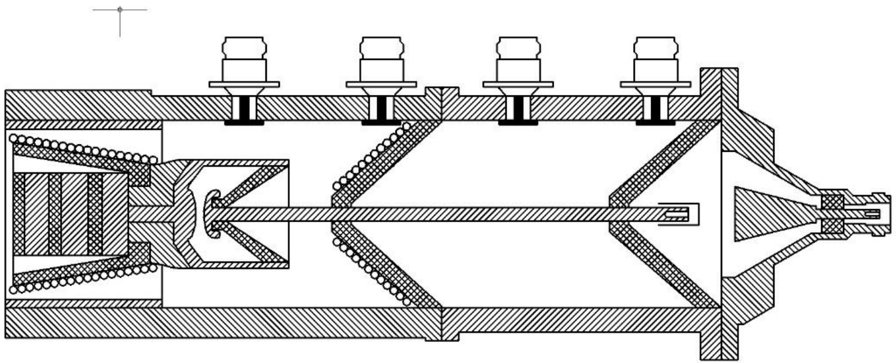

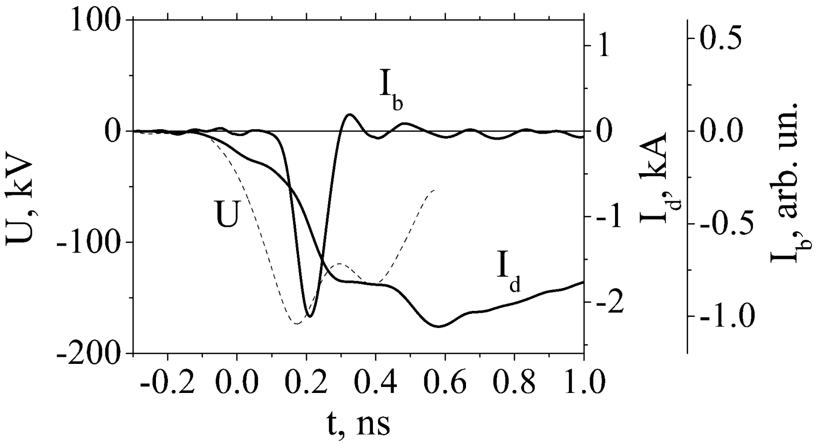

Генерации убегающих электронов (УЭ)

СЛЭП – сверхкороткий лавинный электронный пучок

SAEB – supershort avalanches electron beam

First brilliant idea about runaway electrons

Wilson C. T. R., The Acceleration of *b*-particles in Strong Electric Fields such as those of Thunderclouds // Proc. Cambridge Philos. Soc. 22, 534-538 (1924).

Theory was development

Eddington A. S. The source of stellar energy. Nature, 117 (2948), 25-32. (1926).

Giovanelly R. G., "Electron Energies Resulting from an Electric Field in a Highly Ionized Gas," Philos. Mag. 40, 206 (1949).

Gurevich A. V., and Zybin K. P. Runaway breakdown and electric discharges in thunderstorms, Phys. Uspekhi, 44, 1119–1140 (2001).

Et al.

Runaway electrons

o [*e with energy T_1*] E [kV/cm] $\longrightarrow$ +M = o' [*e with energy T_2*]

$$T_2 = T_1 + eU - T_L > T_1$$

In the upper chromosphere and corona, where the ionization is very high, the currents will not be limited by excitation, and if a field greater than the critical field persists, the electron energy will continue to increase until limited by some additional factor. The drift velocity and hence the conductivity thus becomes extremely large.

Dependence of the ionization frictional force on the electron energy assigned to an electron charge for helium and air at atmospheric pressure.

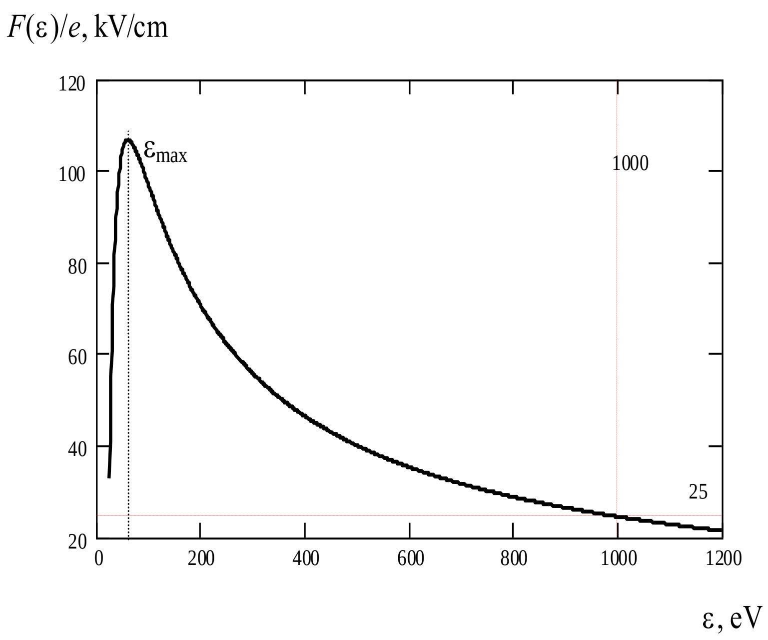

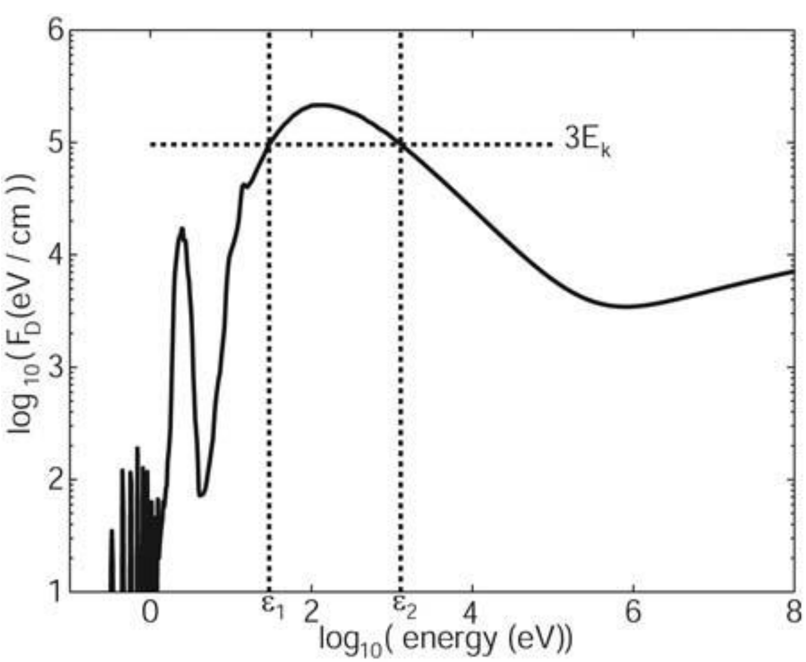

First observation of x-ray from gas diode after anode foil at pressure 1 atmosphere (от идеи прошло более 40 лет)

- Frankel S., Highland V., Sloan T., Van Dyck and Wales W. // Nuclear Instruments and Methods. 1966. V. 44. P.345-348. (He)
- Stankevich Yu.L, Kalinin V.G. // Doklady Akademii Nauk SSSR. 1967. V. 177. No. 1. P. 72-73. (Air)
- R.C. Noggle, E.P. Krider, J.R. Wayland. J. Appl. Phys., 1968. V.39. P.4746-4748. (He) (REP DD)
- Tarasova L.V., Khudjakova L.N. // JTF. 1969. V. 39. No 8. P. 1530-1533. (Air) (REP DD)

First direct measurement of e-beam from gas diode after anode foil at pressure 1 atmosphere (in air, helium, D_2, argon, xenon):

Тарасова Л. В., Худякова, Л. Н., Лойко Т. В., & Цукерман, В. А. Быстрые электроны и рентгеновское излучение наносекундных импульсных разрядов в газах при давлениях 0.1–760 Тор // Журнал технической физики. – 1974. – Т. 44. – №. 2. – С. 564–568.

Обзор основных результатов до 2003 года:

Babich L P 2003 High-Energy *Phenomena in Electric Discharges in Dense Gases: Theory, Experiment and Natural Phenomena* (Arlington, VA: Futurepast.)

Начало нового цикла исследований, 2002 год:

Алексеев С.Б., Орловский В.М., Тарасенко В.Ф. Пучок электронов, сформированный в газонаполненном диоде при атмосферном давлении воздуха и азота // Письма в ЖТФ. – 2003. – Т. 29. – Вып. 10. – С. 29–35

Ткачев А.Н., Яковленко С.И. Механизм убегания электронов в газе и критерий зажигания самостоятельного разряда // Письма в ЖЭТФ. – 2003. – Т. 77. – Вып. 5. – С. 264–269.

Моделирование генерации убегающих электронов при атмосферном давлении с выводом пучка электронов за фольгу

Jiang W., Yatsui K. et al. Numerical simulation of sub-nanosecond electron beam extraction from gas-filled diode // Proceedings of Int. Conf. on High-Power Particle Beams (BEAMS 2004). Saint-Petersburg, 2005. IEEE. 2004 (ISBN 978-5-87911-088-3). P. 174-177.

The distribution of electric field in the gap. "Tube-plane" configuration.

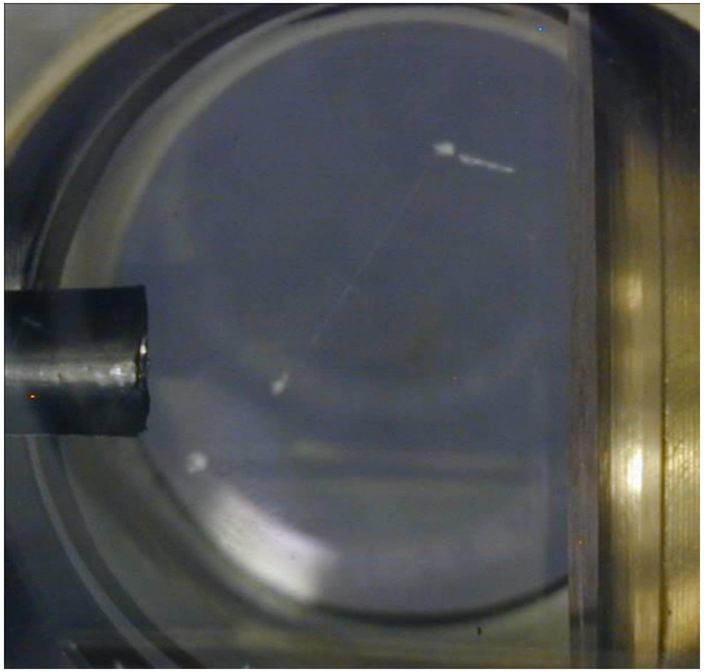

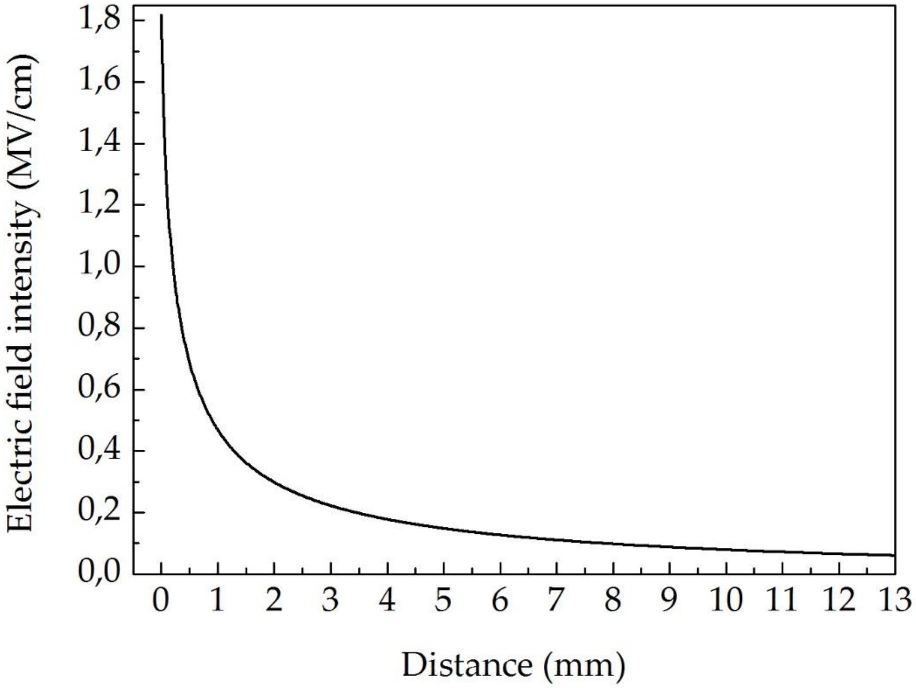

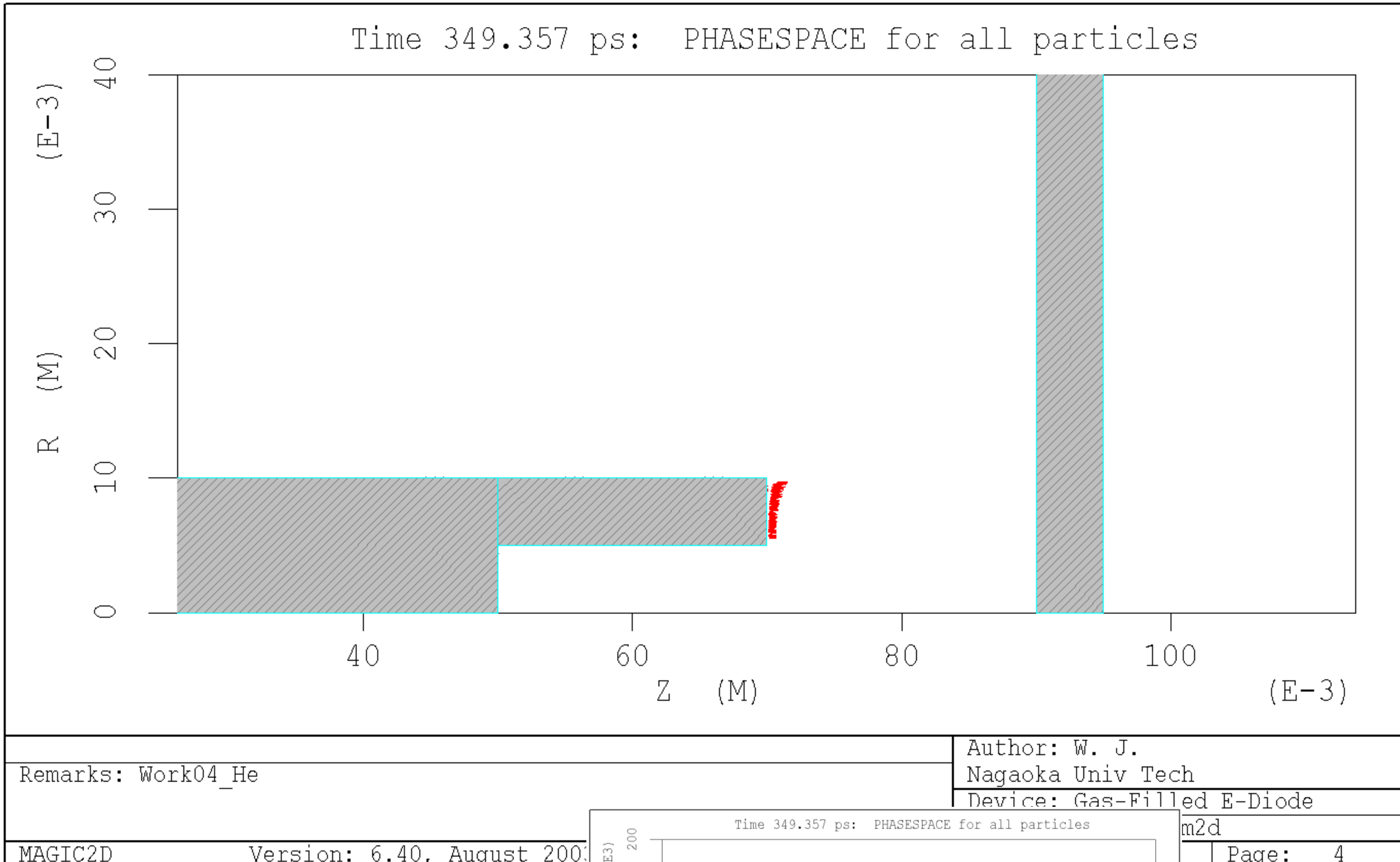

Electron Map (t = 350 ps)

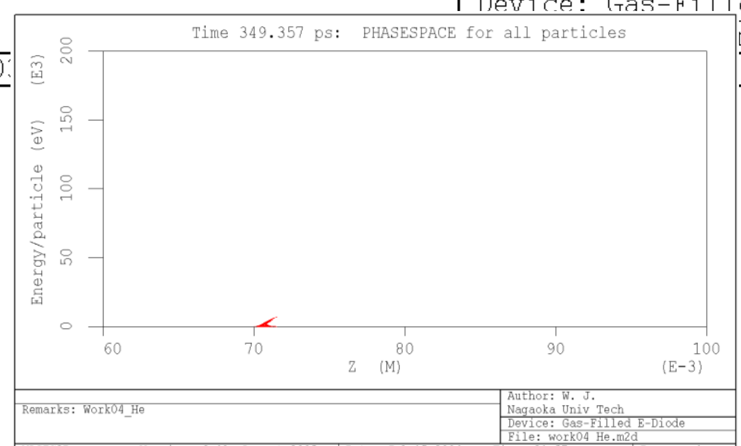

Electron Energy (t = 350 ps)

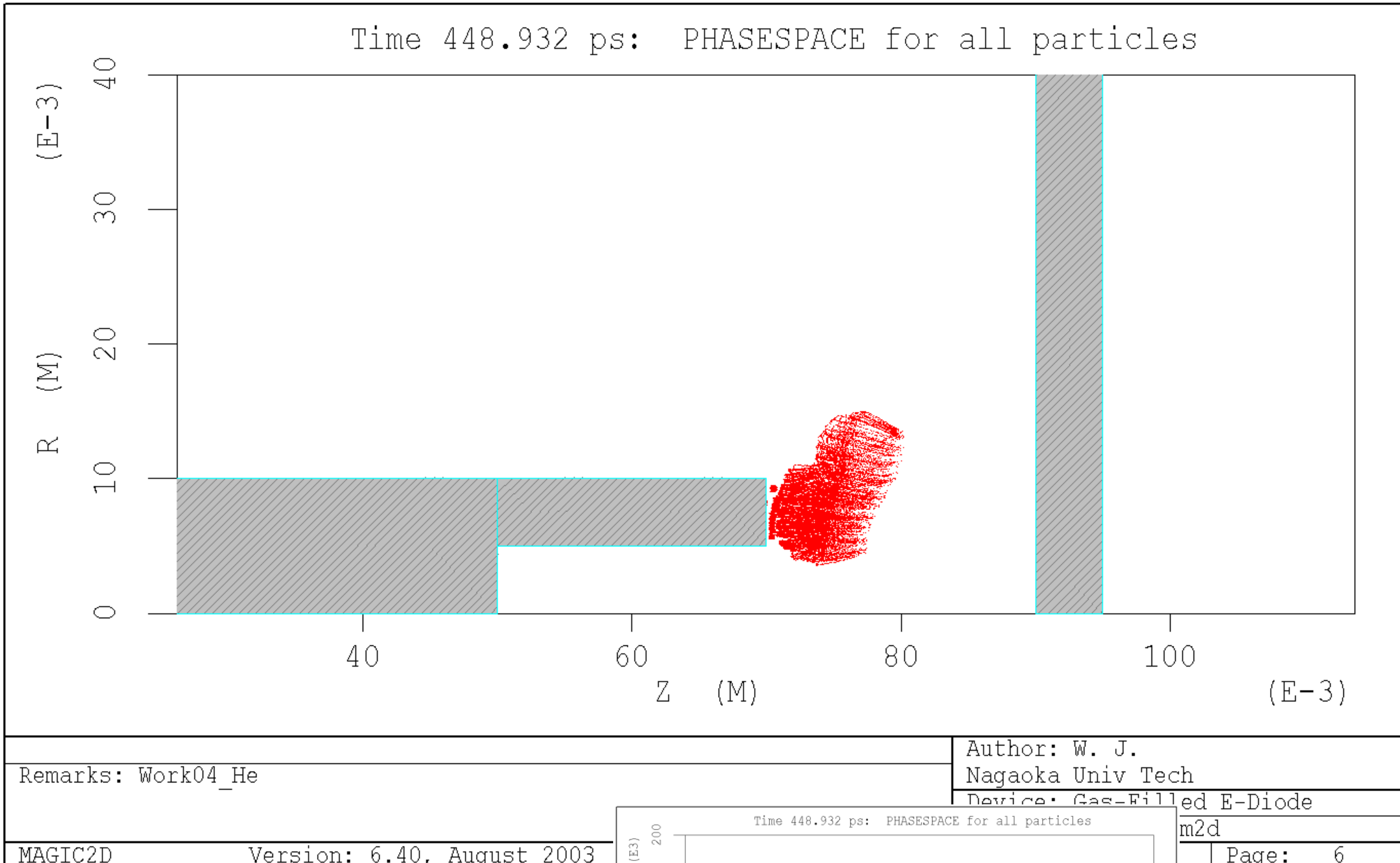

Electron Map (t = 450 ps)

Electron Energy (t = 450 ps)

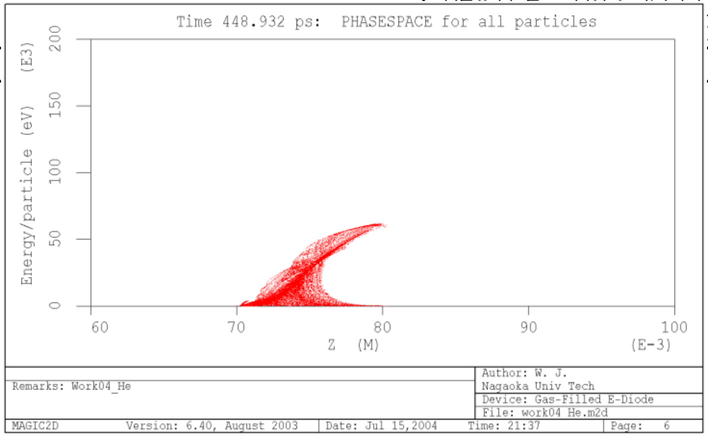

The integral photography of discharge glow. Voltage pulse duration is 0.2 ns. Gap *d* = 16 mm, tube cathode with diameter 6 mm, pulser SLEP-150.

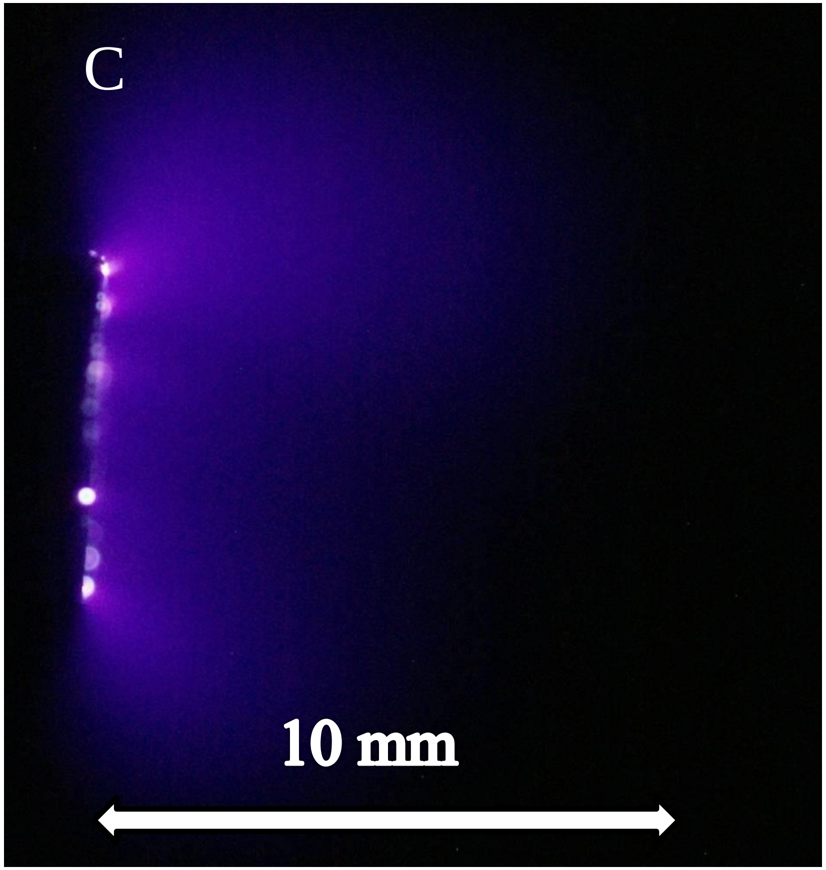

Gap 16 mm

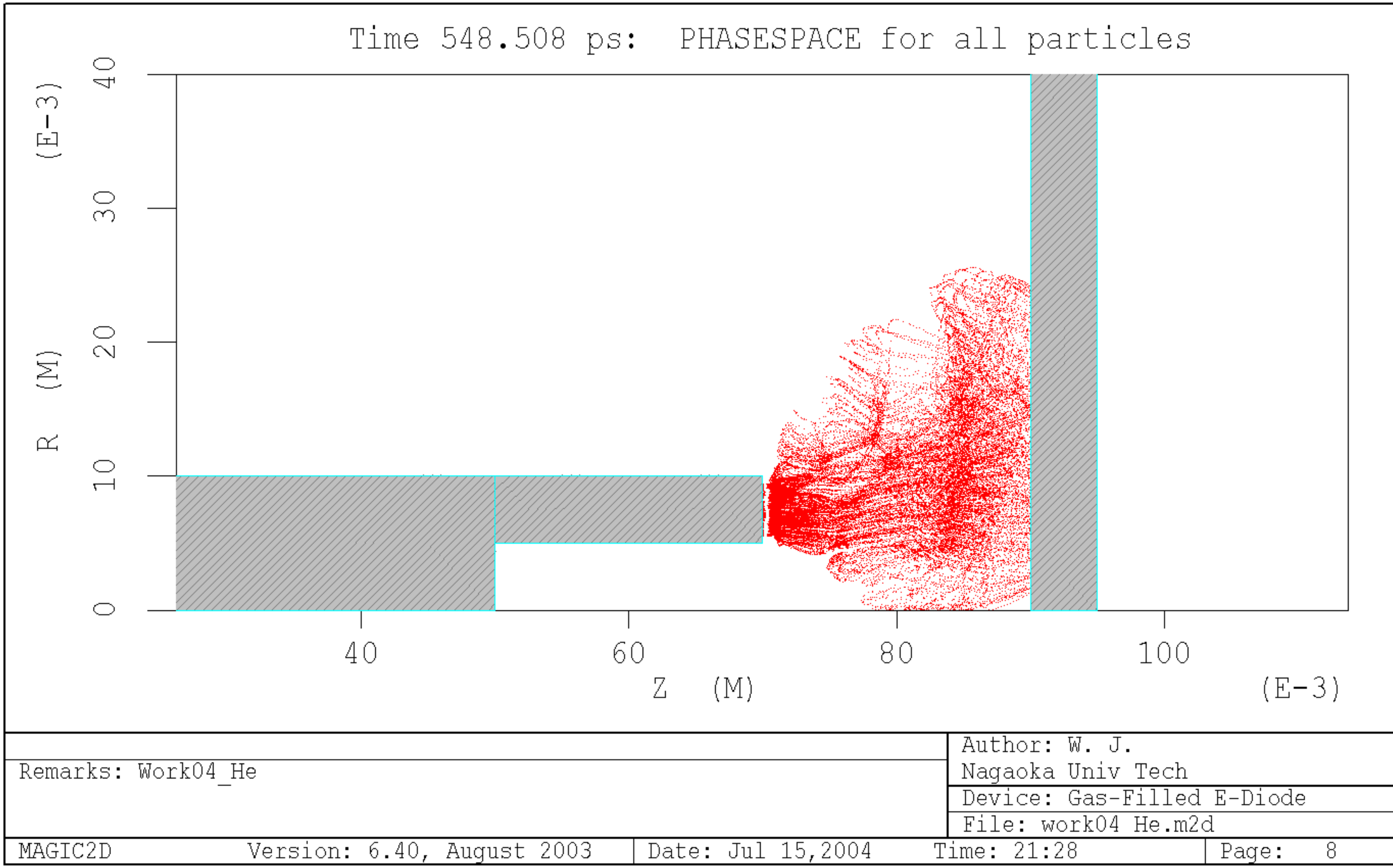

Electron Map (t = 550 ps)

Electron Energy (t = 550 ps)

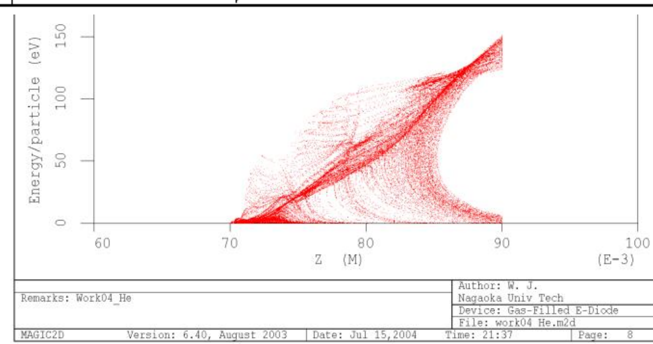

The integral photography of discharge glow. Voltage pulse duration is about 2 ns. Gap *d* = 14 mm, tube cathode with diameter 6 mm. N_2, *p* = 1 atm.

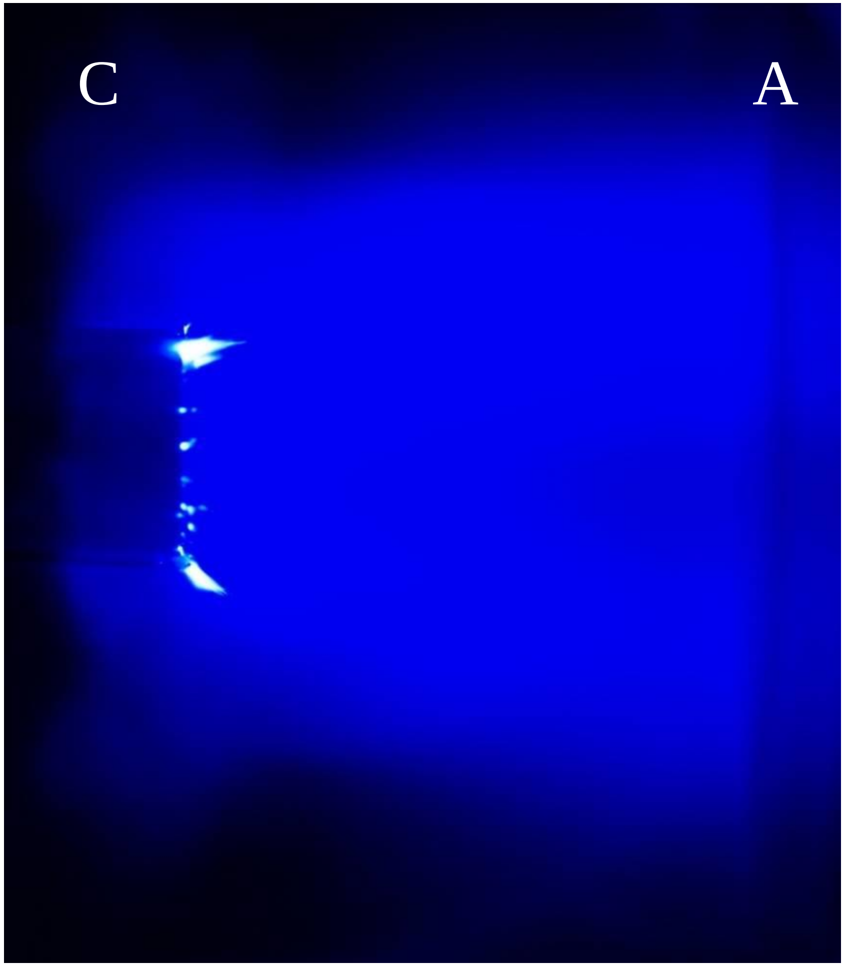

Моделирование условий генерации пучков убегающих электронов (малая часть работ)

1. D. Levko, S. Yatom, V. Vekselman, J.Z. Gleizer, V.T. Gurovich, Y.E. Krasik. J. of Applied Physics, 111 (1), 013304 (2012).
2. Oreshkin, E. V., Barengolts, S. A., Oreshkin, V. I., & Mesyats, G. A. (2017). Parameters of a runaway electron avalanche. *Physics of Plasmas*, *24*(10), 103505.
3. S.Y. Belomyttsev, A.A. Grishkov, V.A. Shklyaev, V.V. Ryzhov. J. of Applied Physics, 123, 043309, (2018).
4. V.Y. Kozhevnikov, A.V. Kozyrev, N.S. Semeniuk, A.O. Kokovin. IEEE Transactions on Plasma Science, 46 (10), 3468 (2018).
5. Н.М. Зубарев, С.Н. Иванов. Физика плазмы, 44 (4), 397 (2018).
6. N.Y. Babaeva, G.V. Naidis, D.V. Tereshonok, E.E. Son. J. of Physics D: Applied Physics 51, 434002 (2018).
7. Levko, D. (2019). Mechanism of sub-nanosecond pulsed breakdown of pressurized nitrogen. *Journal of Applied Physics*, *126*(8), 083303.

Design of the SLEP-150 generator with

a gas diode and a collector (a), and output part of the generator with an additional transmission line, a gas diode and a shunt (b): (1) generator housing, (2) primary winding of the pulse transformer, (3) secondary winding of the pulse transformer, (4) insulator, (5) ferrite rings, (6) dielectric spacer, (7) brass ring, (8) peaking spark gap , (9) capacitive divider U_1, (10) high-voltage coaxial line of wave impedance 30 Ω, (11) short transmission line, (12,19) capacitive divider U_2, (13) discharge gap, (14) connector of the collector, (15) collector receiving part of diameter 20 mm, (16) foil with a diaphragm or a grid, (17) disk cathode with wires, (18,25) inductance for charging the high-voltage coaxial line on the insulator, (20) additional transmission line, (21) capacitive divider U_3, (22) tubular cathode, (23) shunt, (24) insulator.

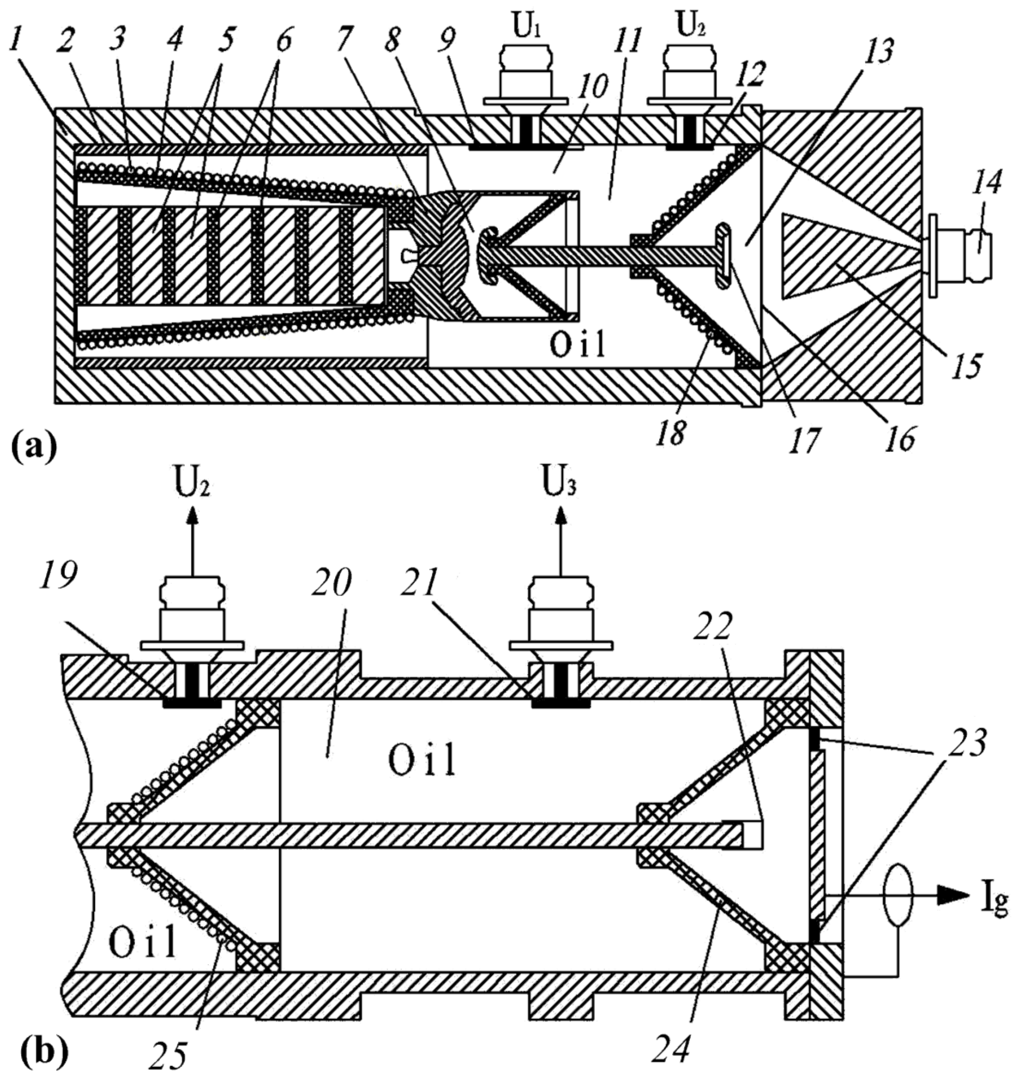

Waveforms of the voltage across the gap *U*, discharge current I_d and electron beam current I_b behind a foil at spherical cathode using. Pulser SLEP-150.

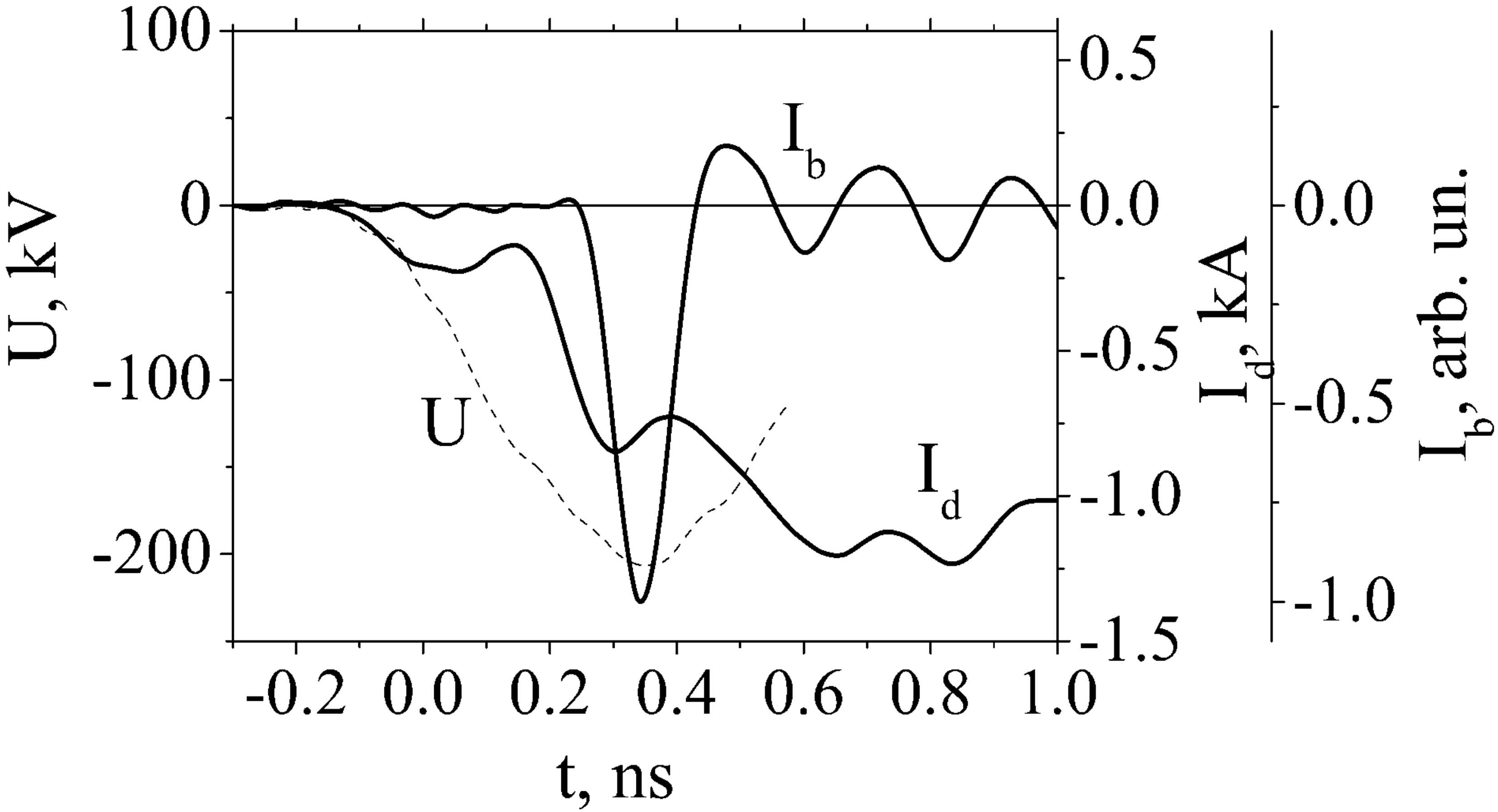

Baksht, E. H., Burachenko, A. G., Kozhevnikov, V. Y., Kozyrev, A. V., Kostyrya, I. D., & Tarasenko, V. F. (2010). Spectrum of fast electrons in a subnanosecond breakdown of air-filled diodes at atmospheric pressure. *Journal of Physics D: Applied Physics*, *43*(30), 305201.

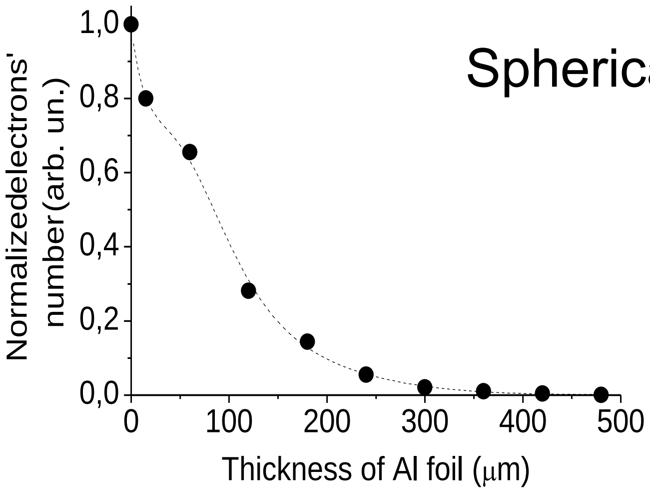

Spherical cathode ∅9,5 mm, gap 8 mm

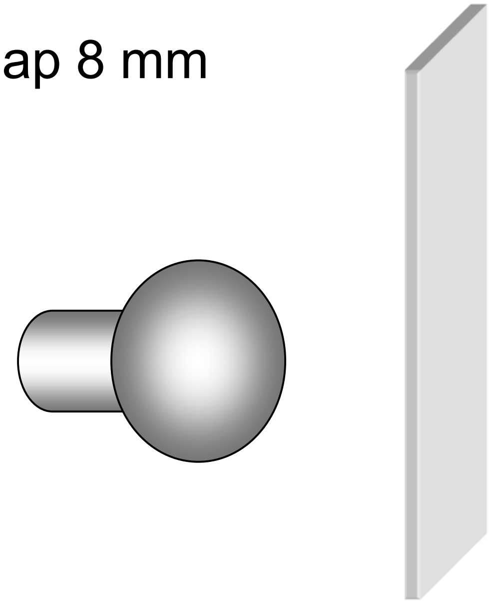

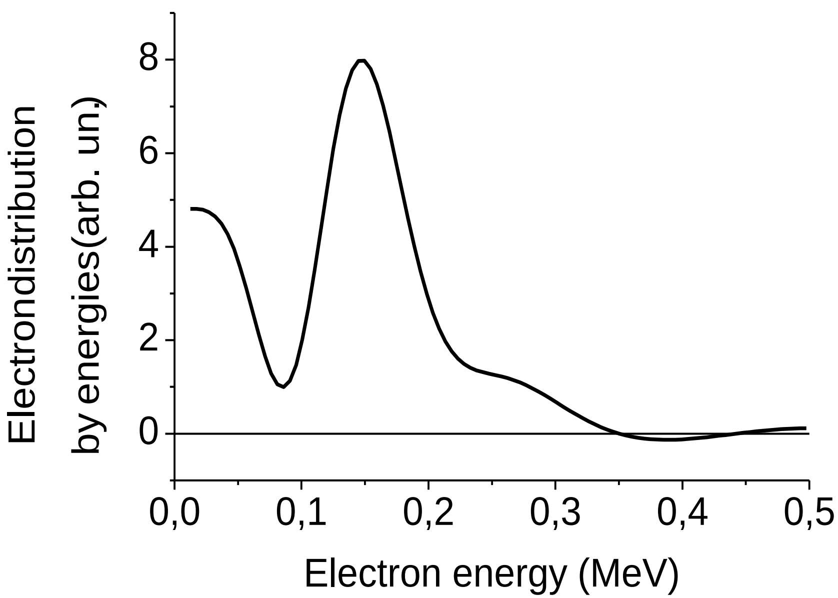

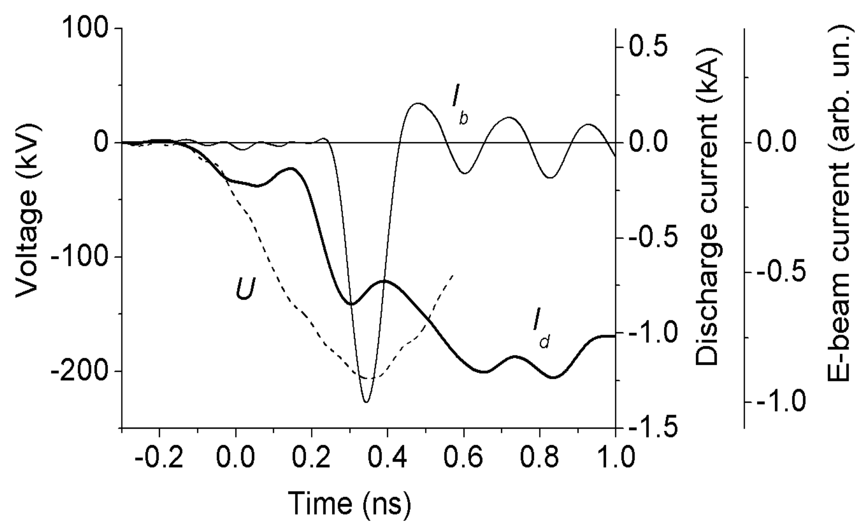

Электроны с «аномальной» энергией ($T>eU$)
Эффект Аскарьяна

1. Аскарьян Г.А. Ускорение частиц краевым полем движущегося плазменного острия // Письма в ЖЭТФ. Т. 1. В. 3. С. 44-49. 1965.
Askar'yan G. A. Acceleration of particles by the edge field of a moving plasma point that intensifies an electric field // Soviet Journal of Experimental and Theoretical Physics Letters. 1965. V. 1. P. 97.

2. Аскарьян Г.А. Самоускорение ионизирующих частиц в электрическом поле ионизирующегося шлейфа ионизации // Письма в ЖЭТФ. Т. 2. С. 179-182. 1965.
Askar'yan G. A. Self-acceleration of Ionizing Particles in an Electric Field of a Polarizing Ionization Loop // Soviet Journal of Experimental and Theoretical Physics Letters. 1965. V. 2. P. 113 – 115.

The optimization of the gap *h* between the wires and the back wall of the cathode and also a decrease in total cathode thickness allow an increase in the number of electrons downstream of the foil. With *h* ~ 1.5 mm, 6.2×10^{10} electrons were detected downstream of the Al foil of thickness 10 μm, which corresponds to a SAEB amplitude of ~100 A with a FWHM of a triangular pulse of 100 ps.

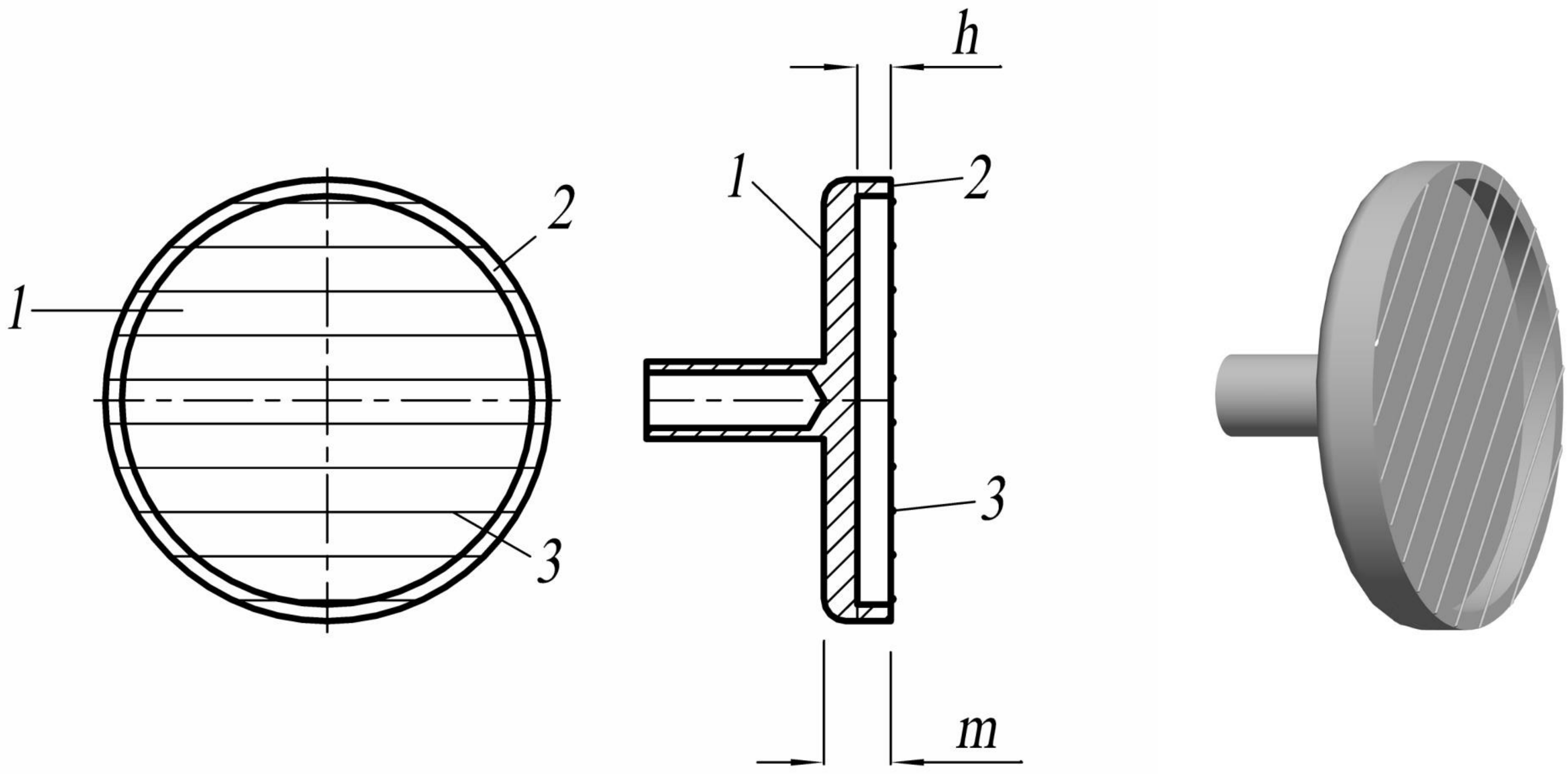

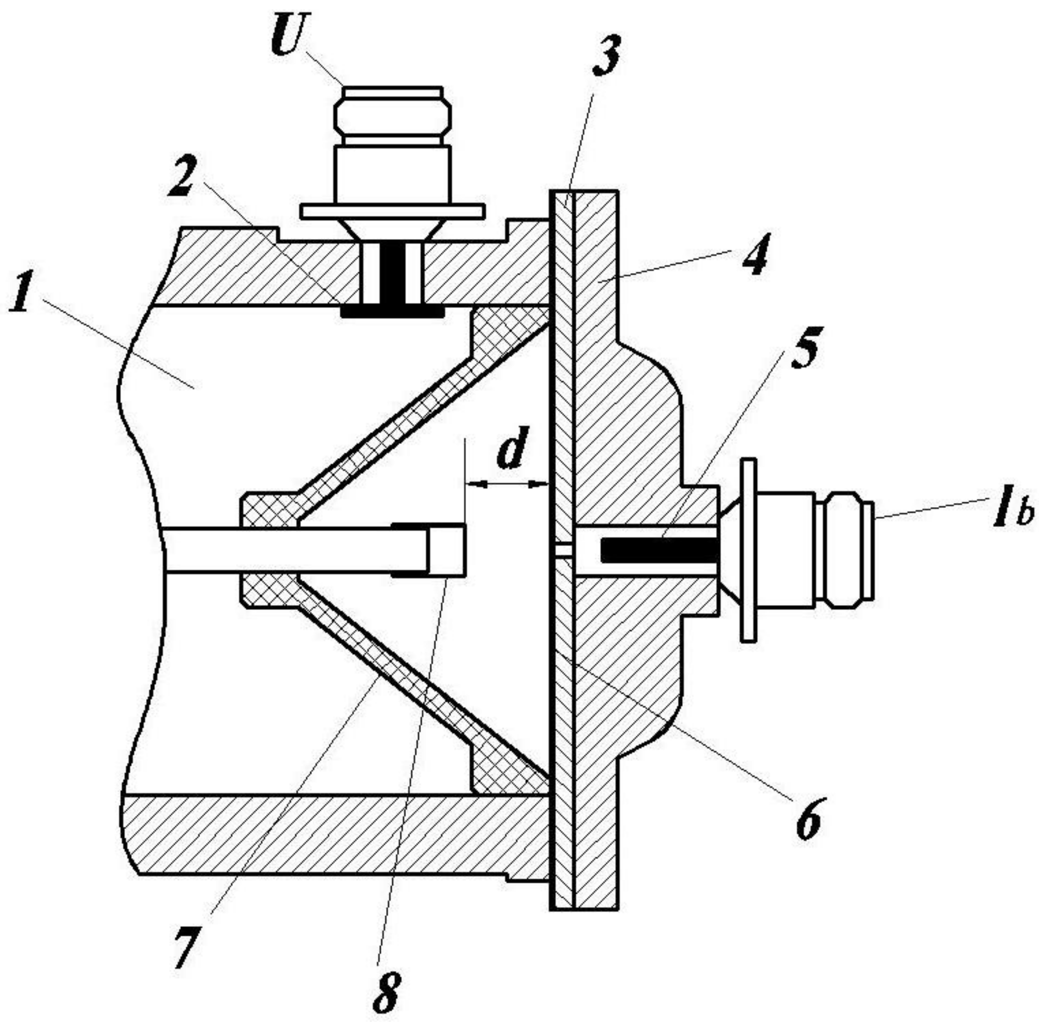

Schematic diagram of SLEP150 generator with gas-filled diode and collector: (1) transmission line; (2) capacitive voltage divider; (3) collimator; (4) collector case; (5) receiving part of the collector; (6) anode foil; (7) diode insulator; (8) cathode (tube).

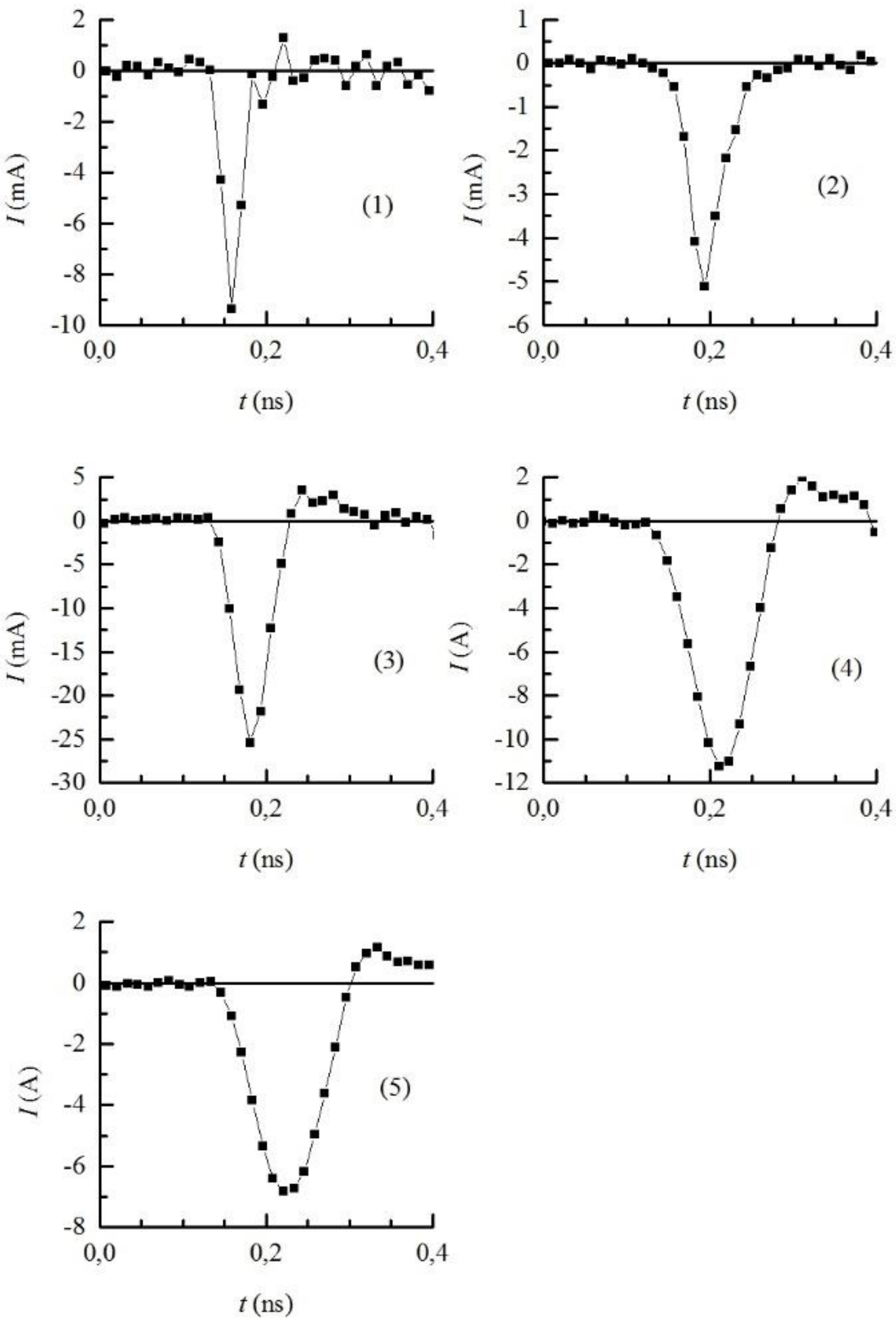

SAEB current pulse oscillograms for (1) ball-shaped cathode with interelectrode gap width of d = 6 mm (25 ps) and (2–5) the cathode tube and an interelectrode gap of 12 mm. The collector had the receiving part with the diameter of (1–3) 3 and (4, 5) 20 mm. The diameter of the hole in the collimator was (1, 2) 1, (3) 4, and (5) 18 mm.

LeCroy WaveMaster 830Zi-A (30 GHz, 80 GS/s) oscilloscope.

Amplitude (*1*) and FWHM (*2*) of the beam current pulse versus the hydrogen pressure. RADAN-220 pulser.

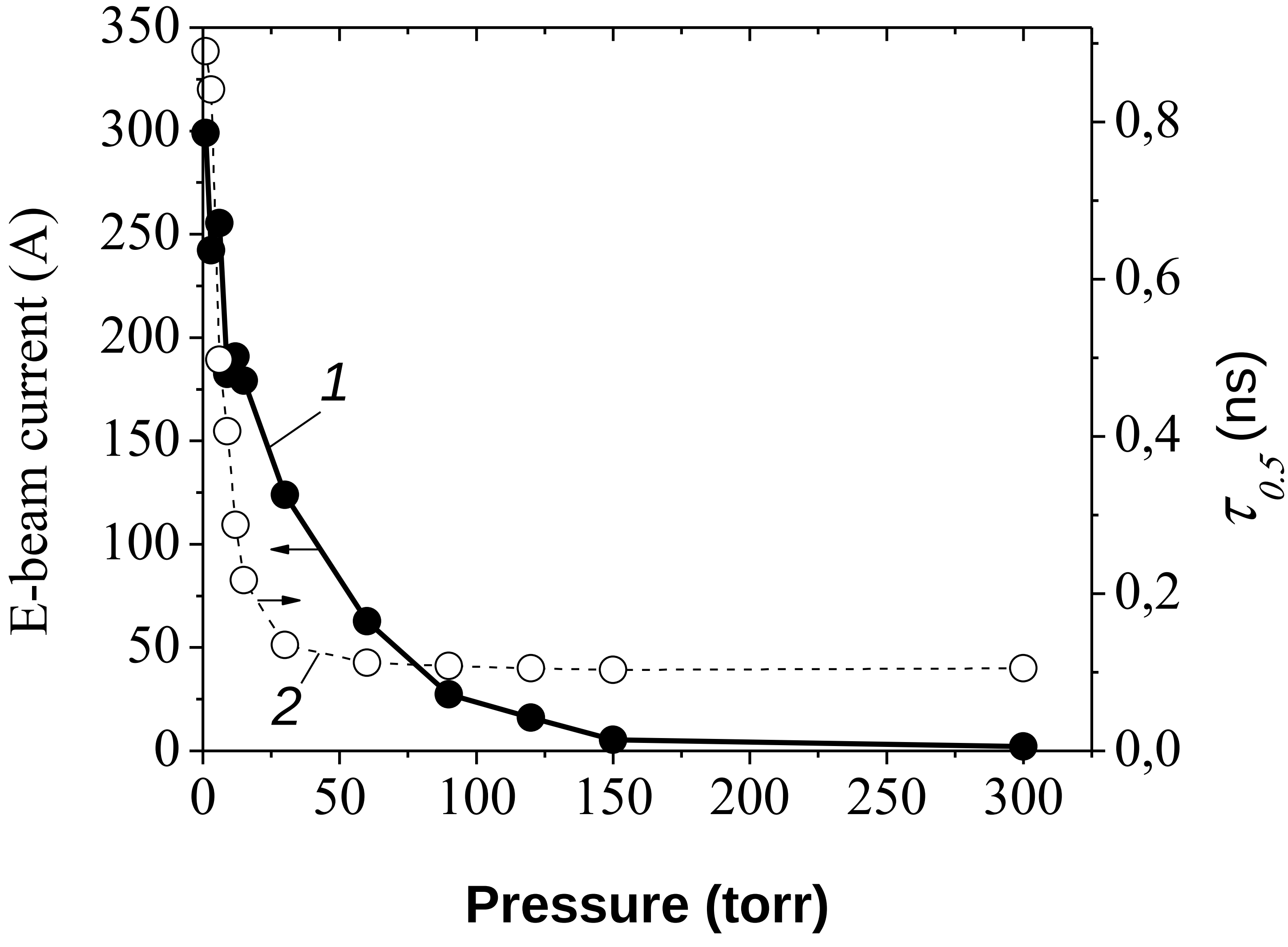

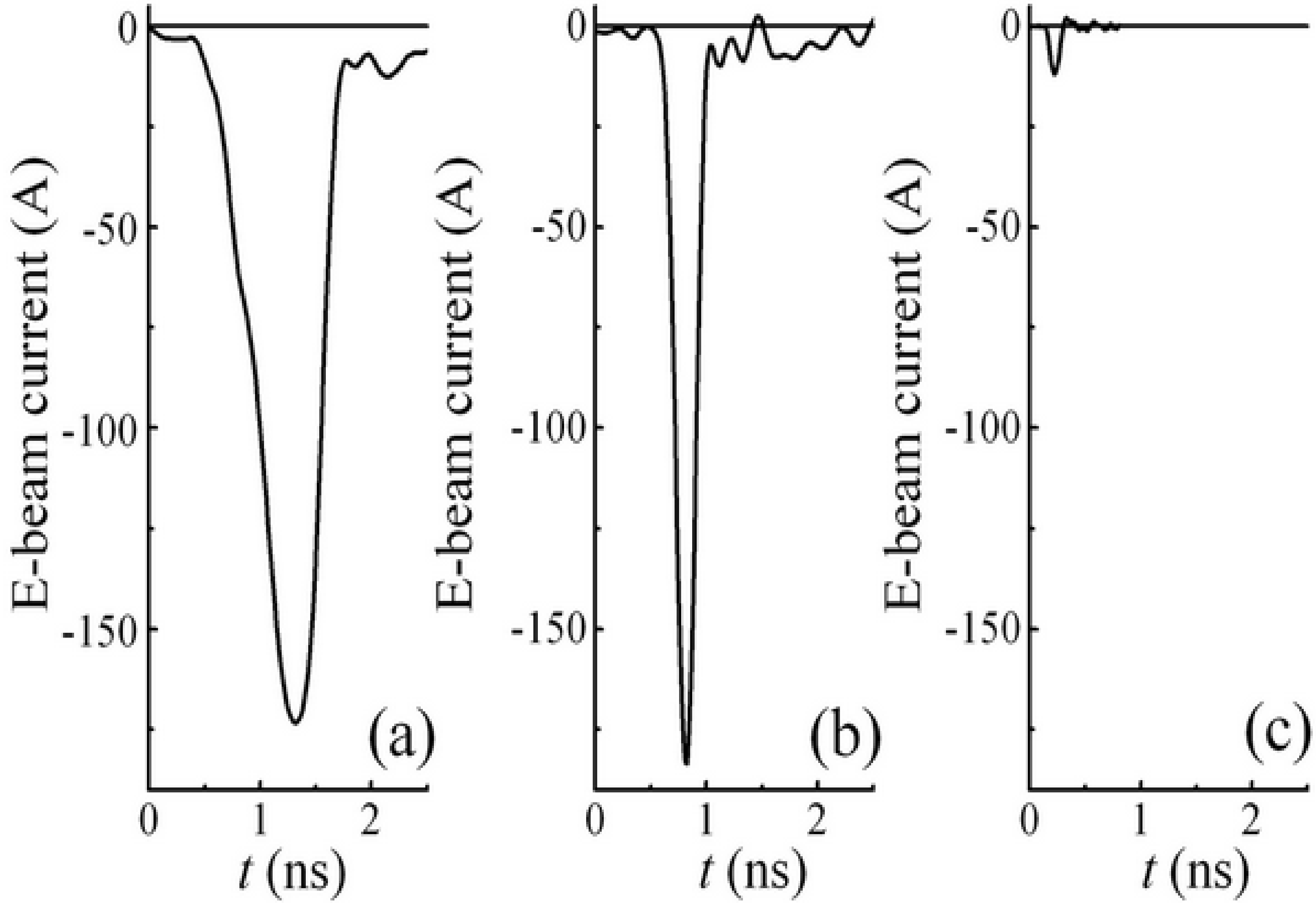

SAEB current measured downstream of a diaphragm 1 cm in diameter at a helium pressure of 9 Torr (a), 60 Torr (b), and 760 Torr (c); tubular cathode, interelectrode gap *d* = 14 mm.

SAEB amplitude vs different gases pressure (up to 1.2 MPa).

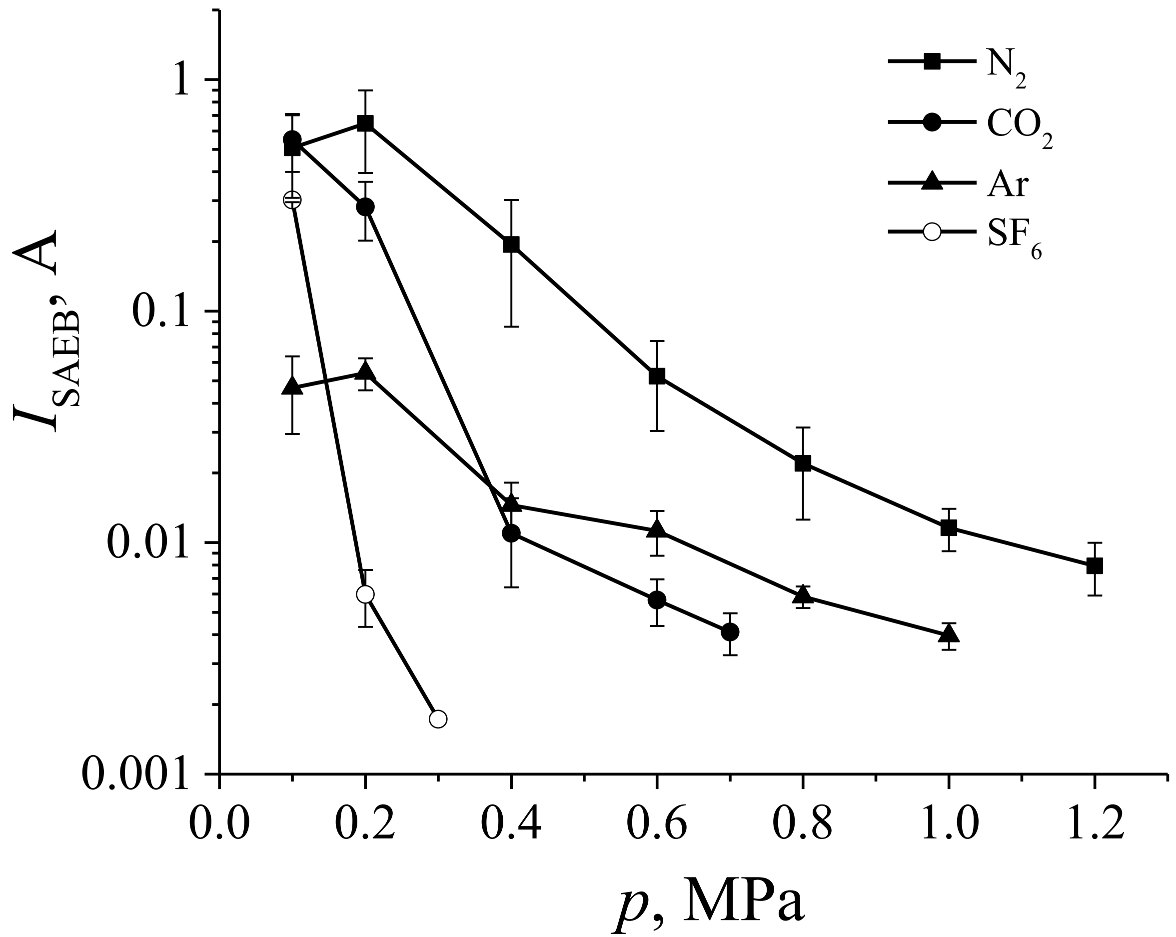

Tarasenko, V. F., Baksht, E. K., Beloplotov, D. V., Burachenko, A. G., Sorokin, D. A., & Lomaev, M. I. (2018). Generation and registration of runaway electron beams during the breakdown of highly overvoltaged gaps filled with dense gases. *Journal of Physics D: Applied Physics*, *51*(42), 424001.

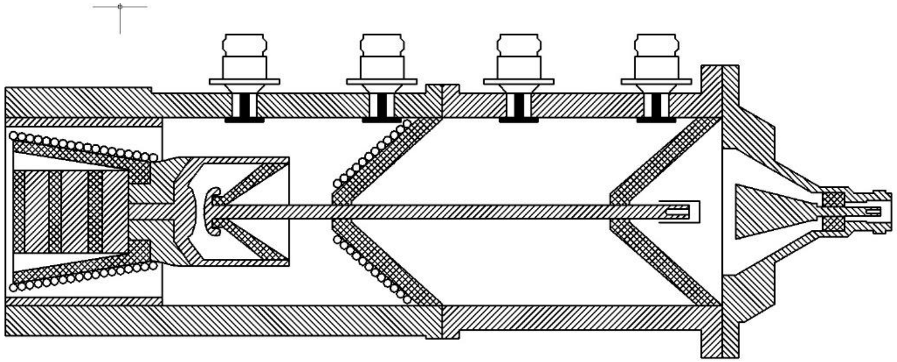

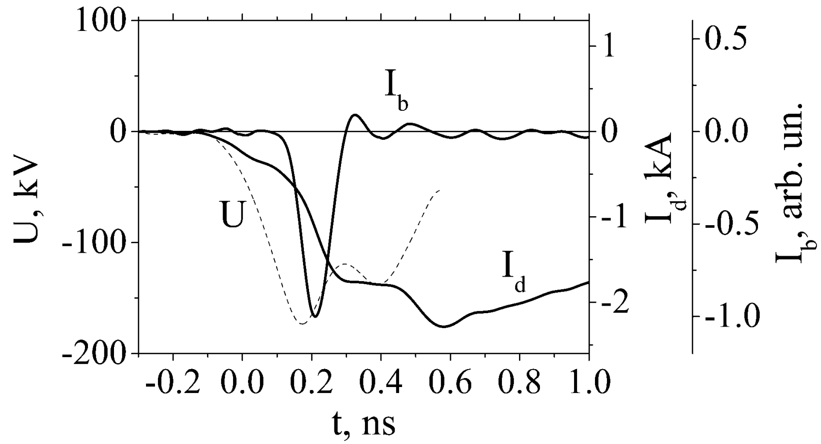

Формирование диффузных разрядов (ДР) в результате стримерного пробоя

REP DD – runaway electron preionized diffuse discharge

ОРИПЭЛ – объёмный разряд инициируемый пучком электронов лавин

First observation diffuse discharge together with x-ray from gas diode after anode foil at pressure 1 atmosphere

- **R.C. Noggle, E.P. Krider, J.R. Wayland. J. Appl. Phys., 1968. V.39. P.4746-4748. (He) (REP DD)**
- **Tarasova L.V., Khudjakova L.N. // JTF. 1969. V. 39. No 8. P. 1530-1533. (Air) (REP DD)**

CO_2 – лазер с катодом из 100 острий

(рентген не регистрировали)

Dumanchin, R., & Rocca-Serra, J. (1969). Augmentation de l’enérgie et de la puissance fournie par unité de volume dans un laser à CO2 en régime pulsé. *CR Acad. Sci.*, *269*(3), 916-917.

Argon

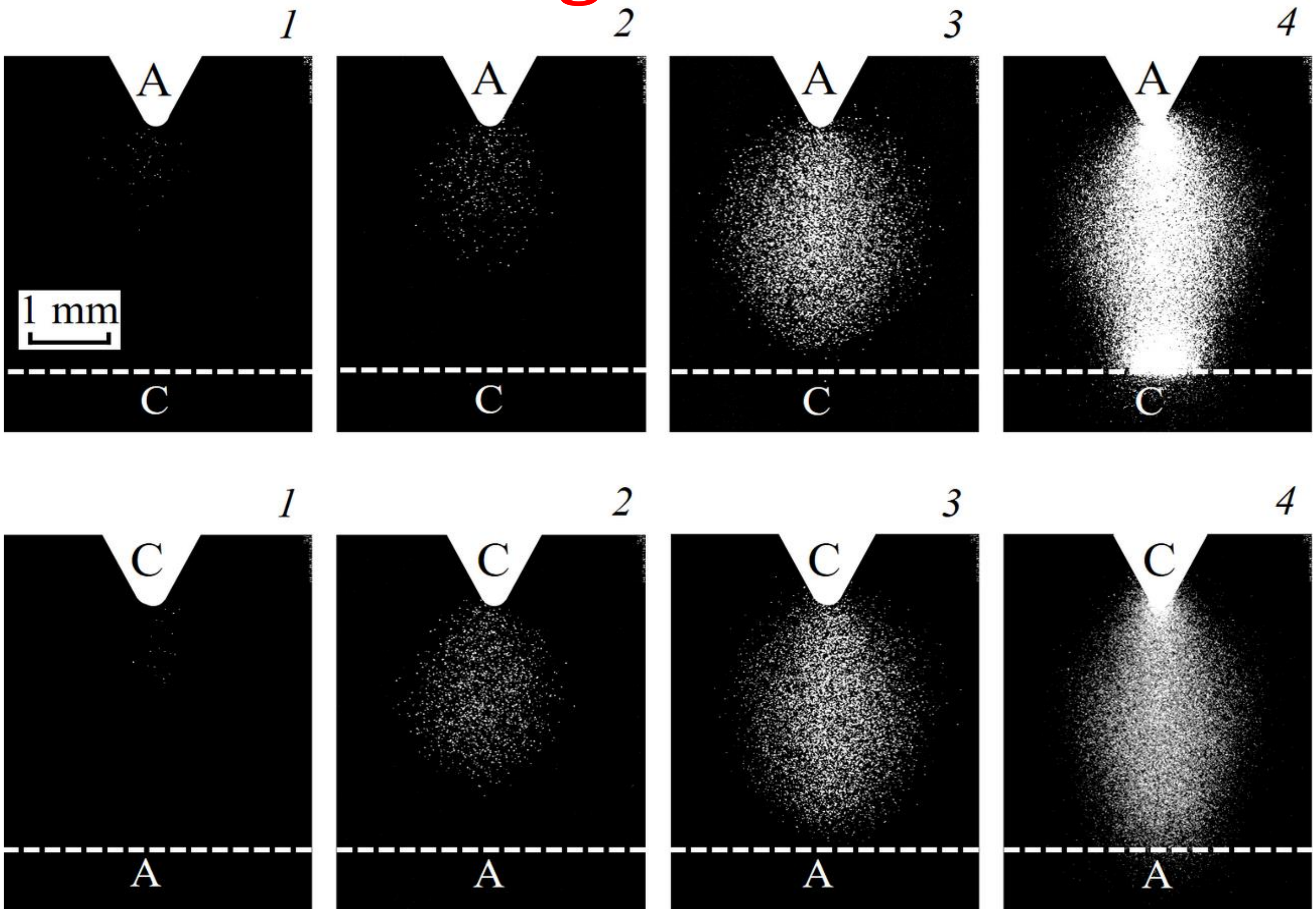

Images of the discharge plasma glow taken with the ICCD camera during first ns. Argon pressure is 100 kPa. Positive and negative polarities. Cone cathode, flat anode. *d* = 3 mm.

Here, (A) is the anode and (C) is the cathode.

Зажигание коронного разряда

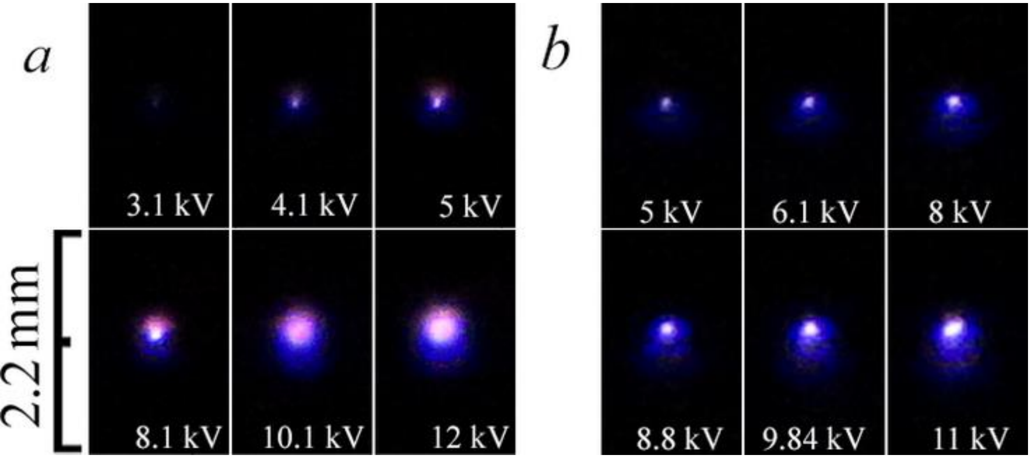

Images of corona discharges near needle No. 1a at negative (a) and positive polarity (b). Length of gap 2 cm. Exposure time 15 s.

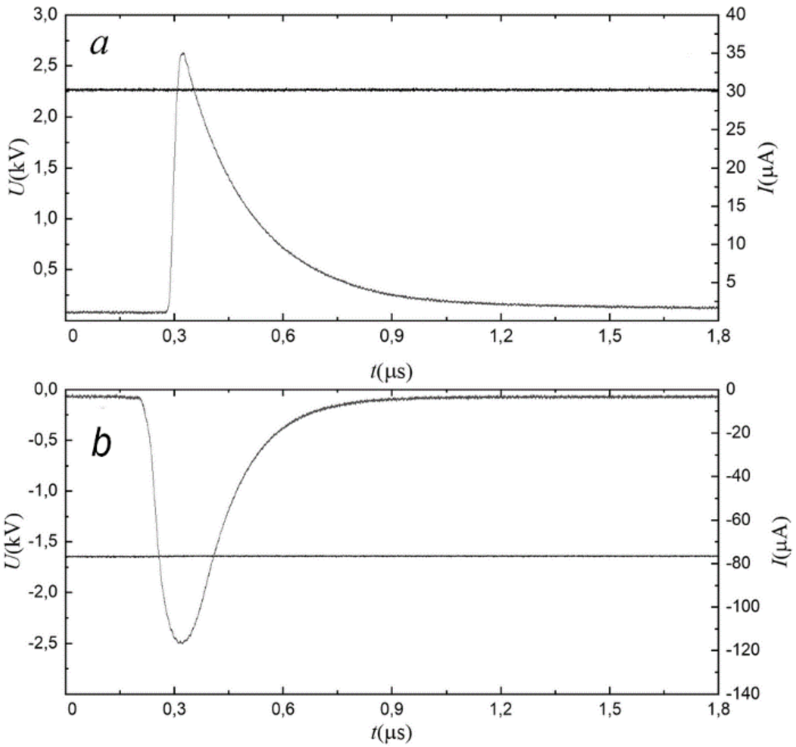

First current pulses (a, b) at different voltages (straight lines) at positive (a) and negative polarity (b). Gaps 5 mm. Needle No. 1b.

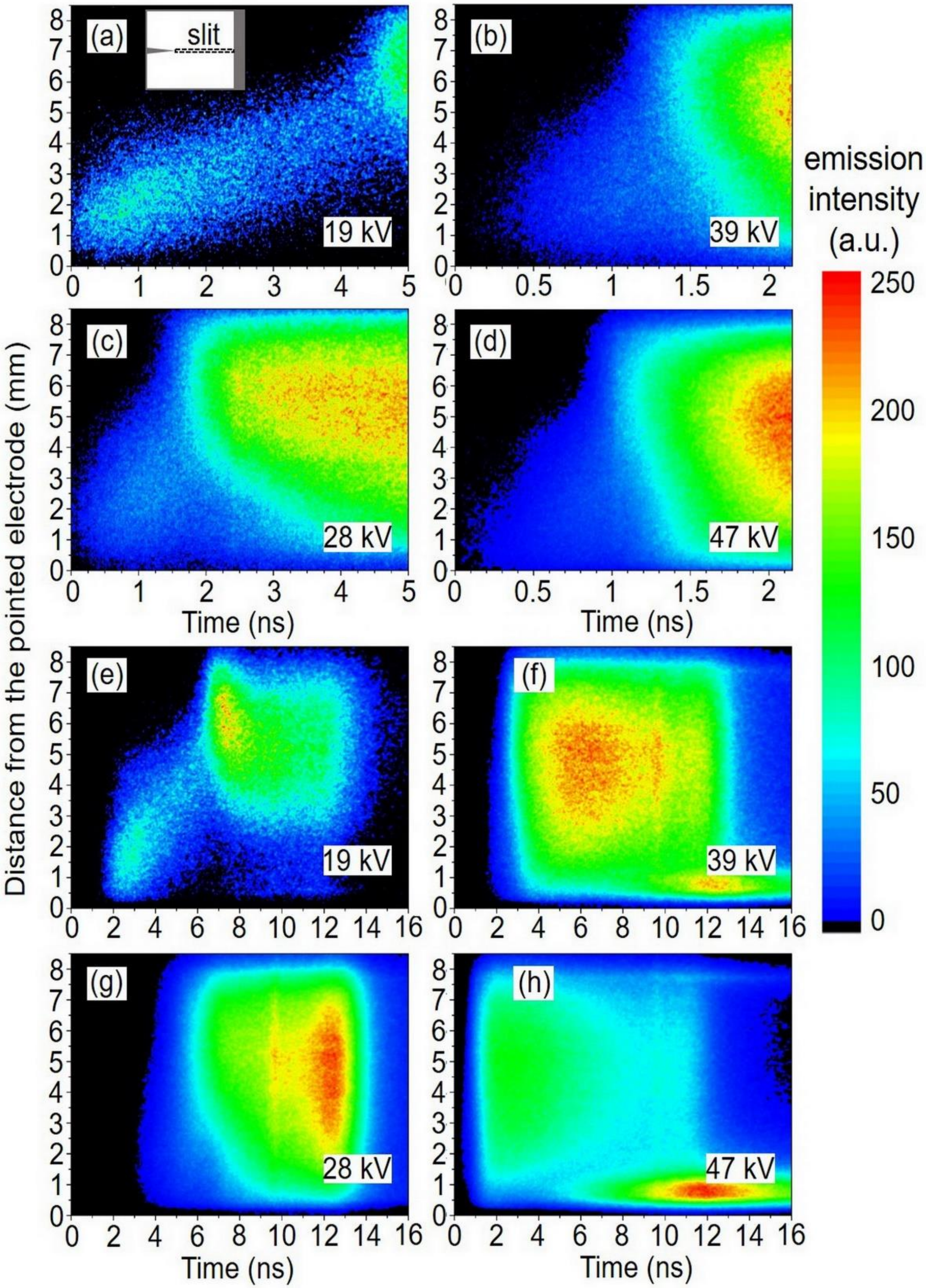

Streak images of the discharge emission in atmospheric-pressure air at various voltages of positive polarity as well as at various sweeps. Setup 1.

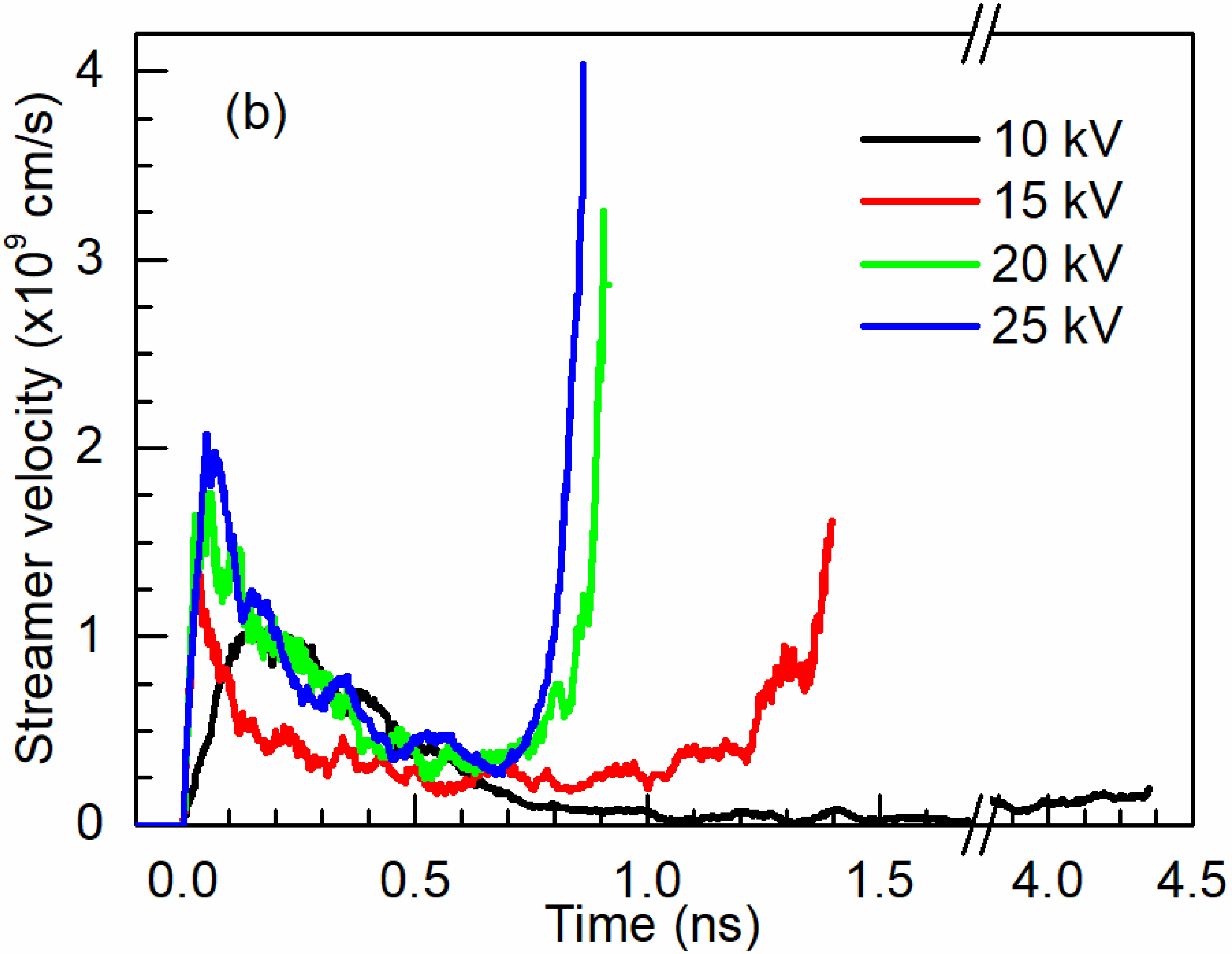

Streak camera image illustrating the propagation of a positive streamer (its glow) along the gap at U_0 = 10 kV.
(b) The time behavior of the streamer velocity $v_{str}(t)$ at U_0 = 10, 15, 20, and 25 kV. Needle high-voltage electrode, atmospheric-pressure air, d = 8.5 mm.

Discharge chamber and photos in nitrogen.
l = 35 cm, *f* = 2 kHz, *d* = 6 mm, *p* = 760 Torr.

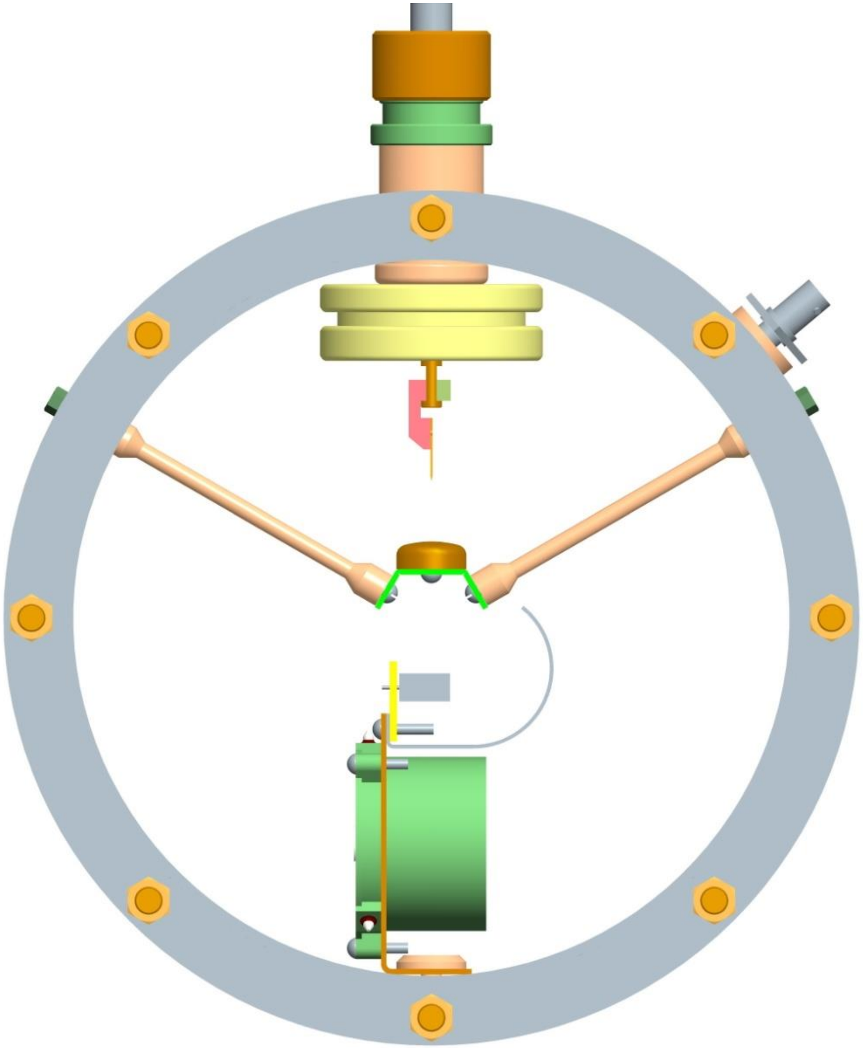

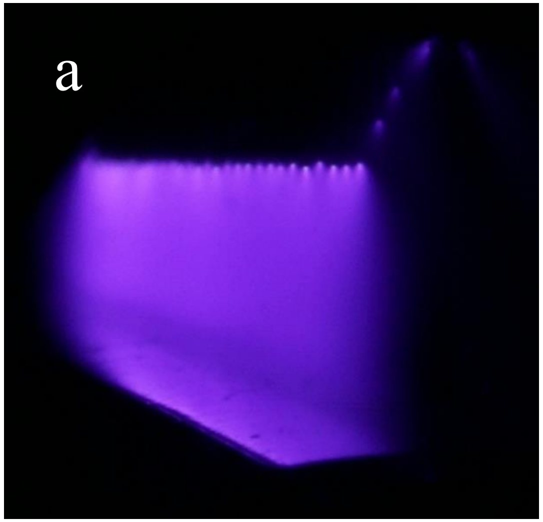

He, 6 atm

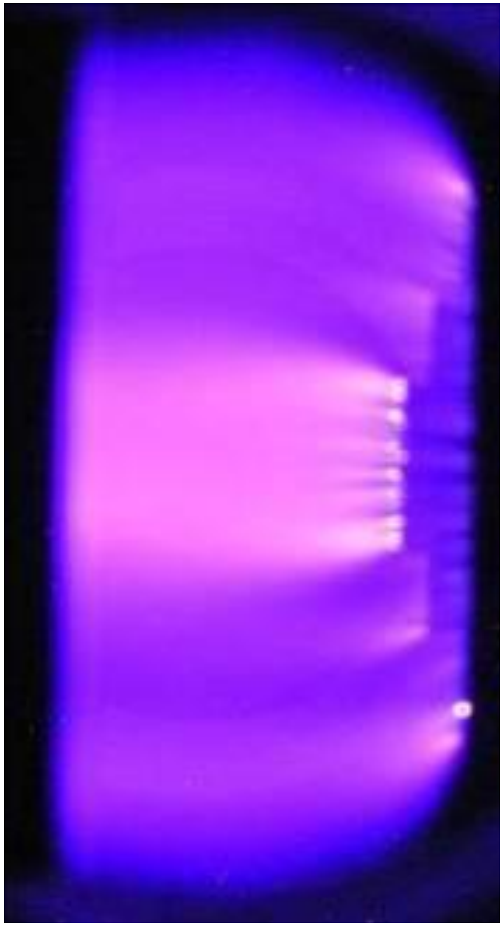

He, 15 atm

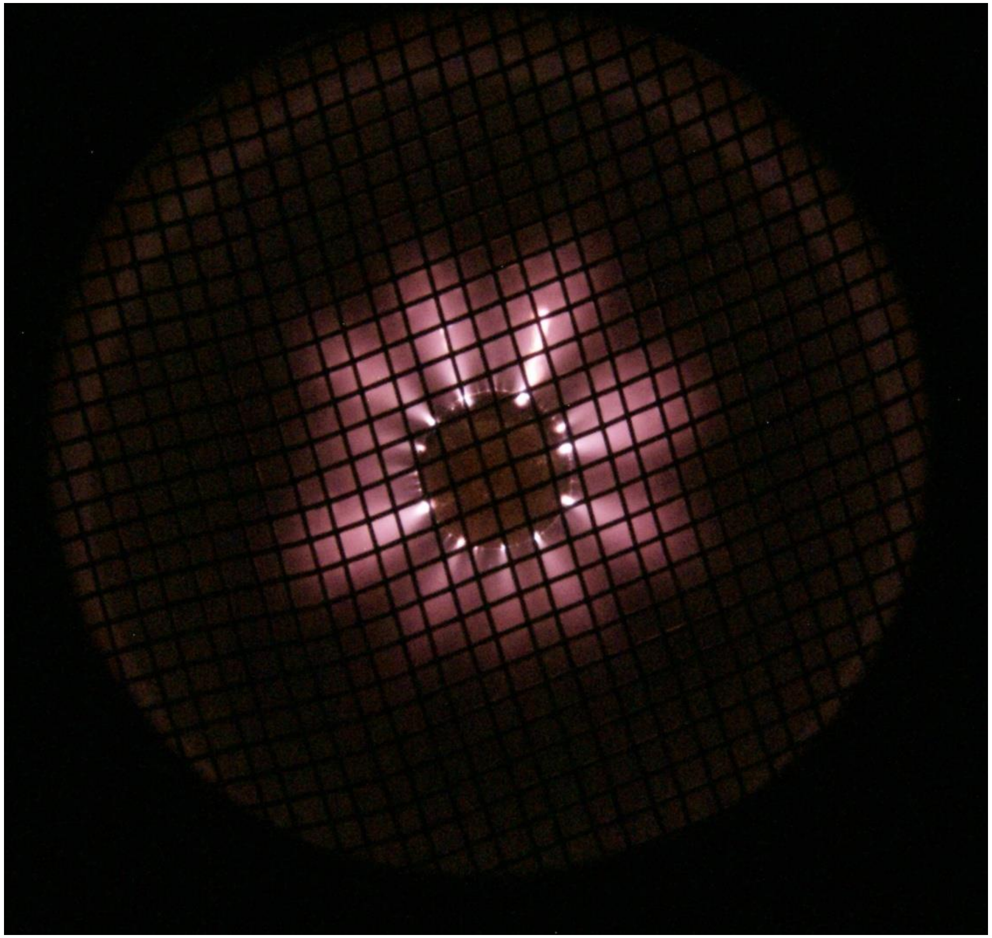

Nitrogen

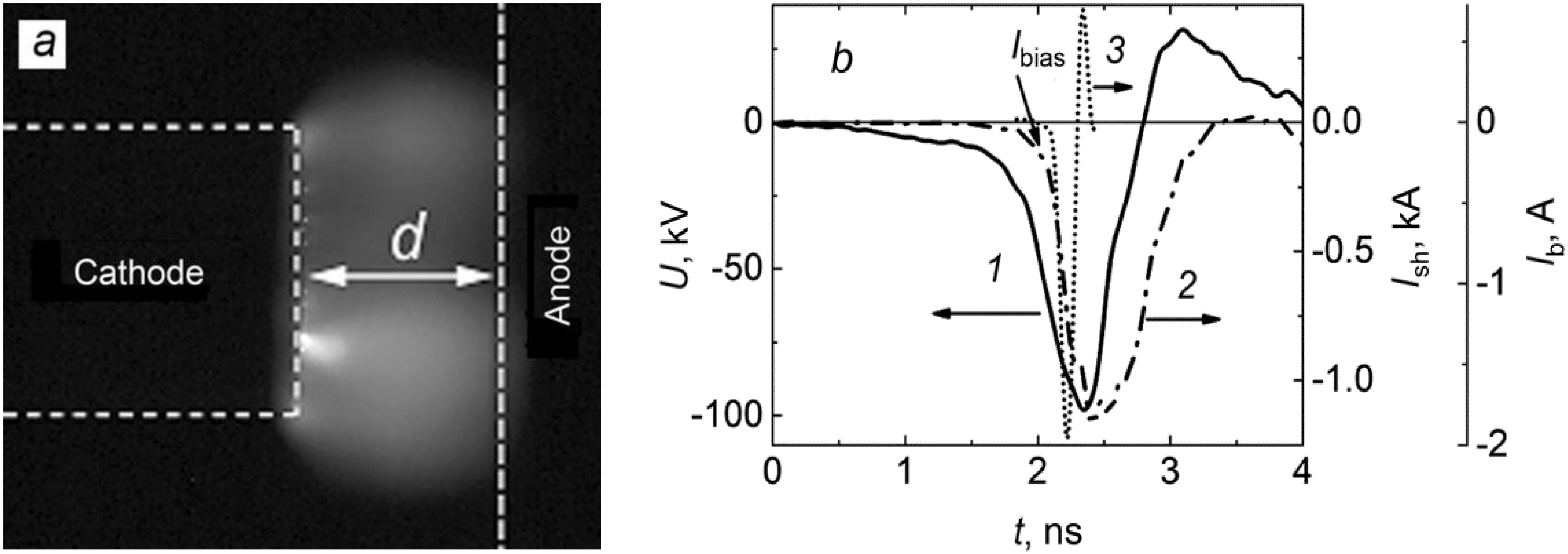

Integral image of the discharge plasma glow (*a*). Waveforms of the voltage pulses *U* (curve *1*), discharge current *I*sh (curve *2*), and super short avalanche electron beam (SAEB) current *I*b (curve *3*) (b). *I*bias – capacitive current from the 'cold cathode' (bias current). Interelectrode spacing *d* = 5 mm. Nitrogen pressure 0.1 MPa. Sleeve potential cathode. Grounded anode – metal disc (*a*) and Al-foil 10 µm in thickness reinforced by the grid with light transmittance 64%) (*b*). Generator – GIN-55-01. Pulse repetition frequency 1 Hz.

Nitrogen

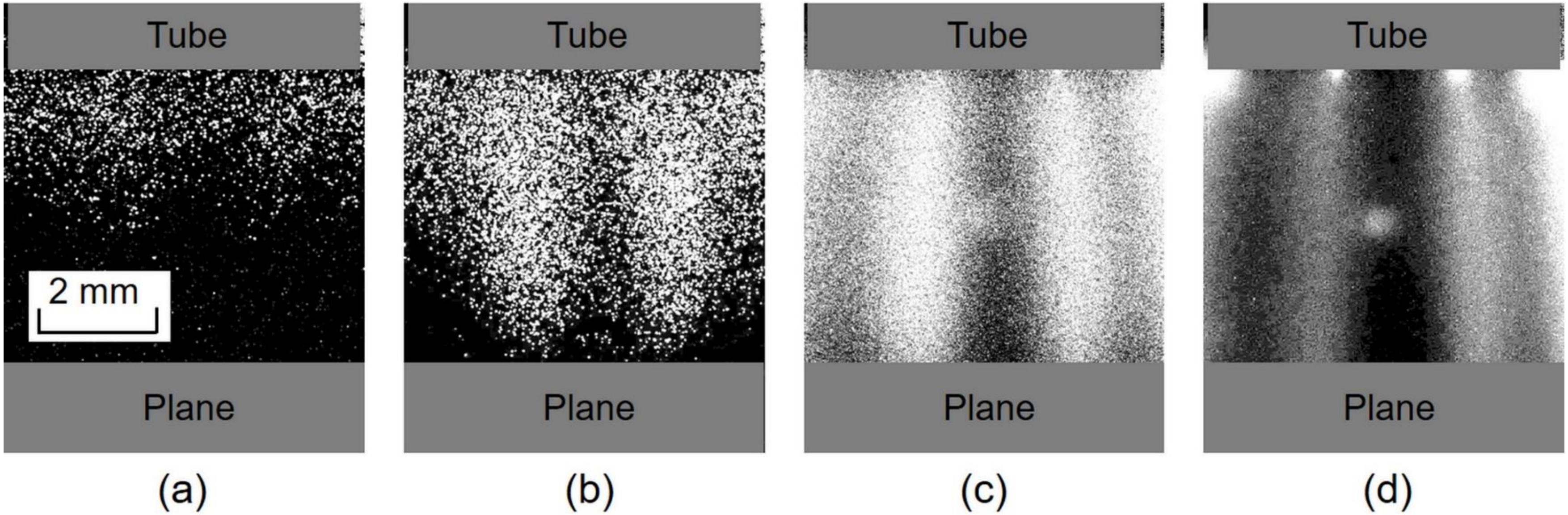

ICCD images of a discharge plasma glow at nitrogen pressure of 0.1 MPa in one pulse of voltage. (a) – 0.2 ns, (b) – 0.4 ns, (c) – 1 ns and d – 10 ns images taken with the ICCD camera. U_p = 20 kV. d = 5 mm. Tubular cathode.

Integral images of plasma glow at discharge in nitrogen at pressures of 0.1 (a) MPa. U_p = 20 kV, d = 5 mm. Tubular cathode.

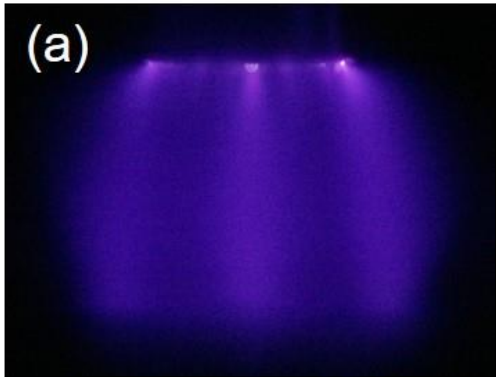

Переход диффузного разряда в искровую стадию с чёточной структурой

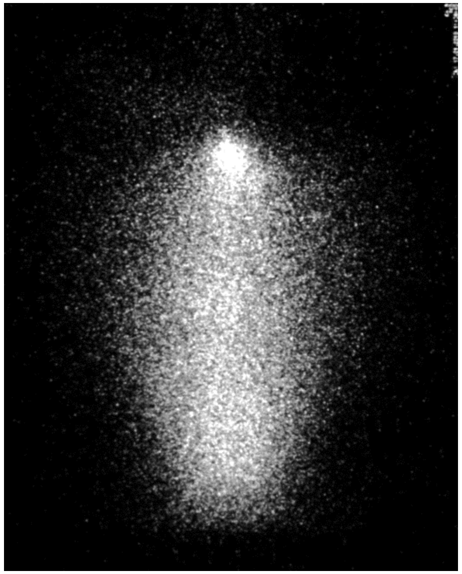

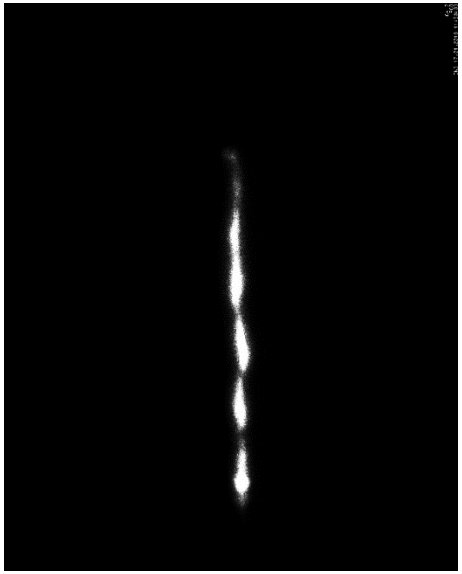

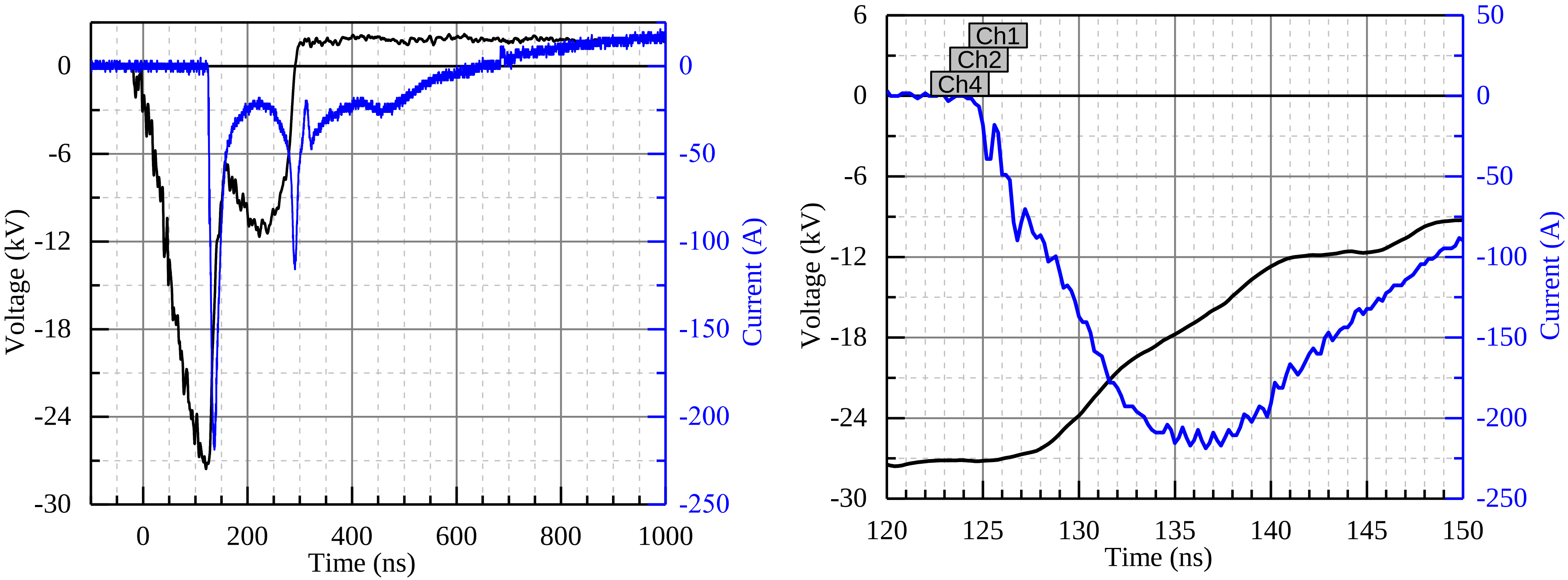

Waveforms of voltage (black) and discharge current pulses (blue).
Air pressure is 100 kPa. d = 8.5 mm.

Air pressure is 100 kPa. *d* = 8.5 mm.

C4 C2 C1 C3

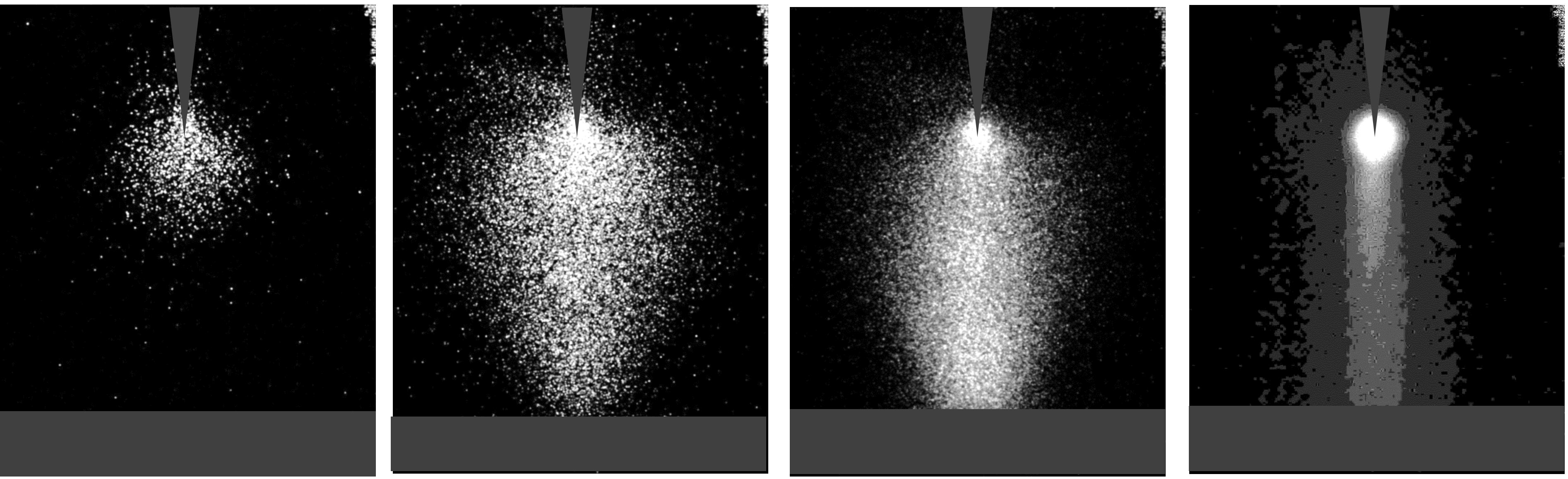

Delay = 4 ns Delay = 5 ns Delay = 6 ns Integr. 30 ns

Images of the discharge plasma glow taken with the ICCD camera. Катод вверху

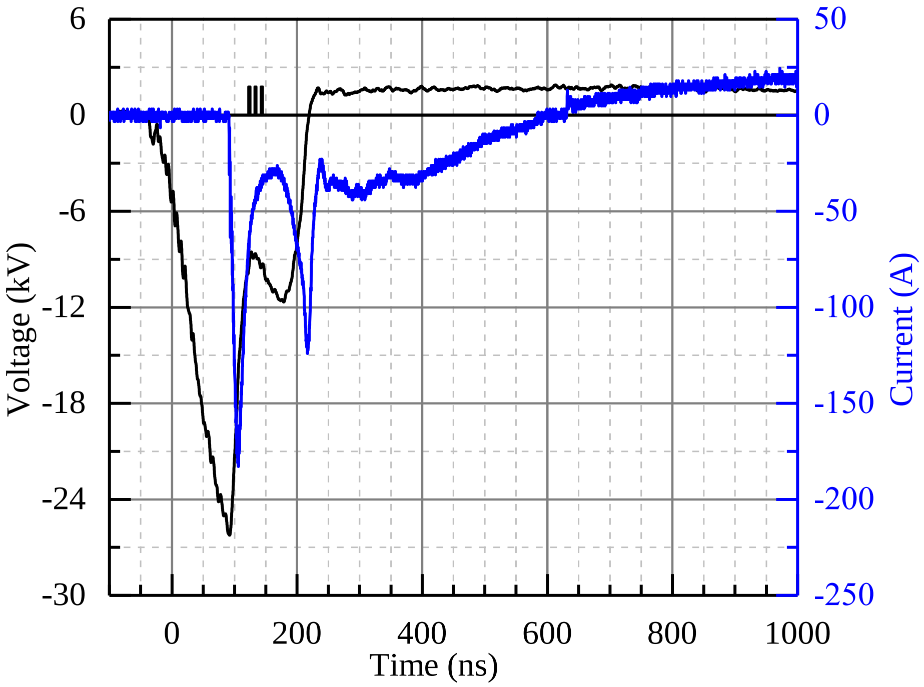

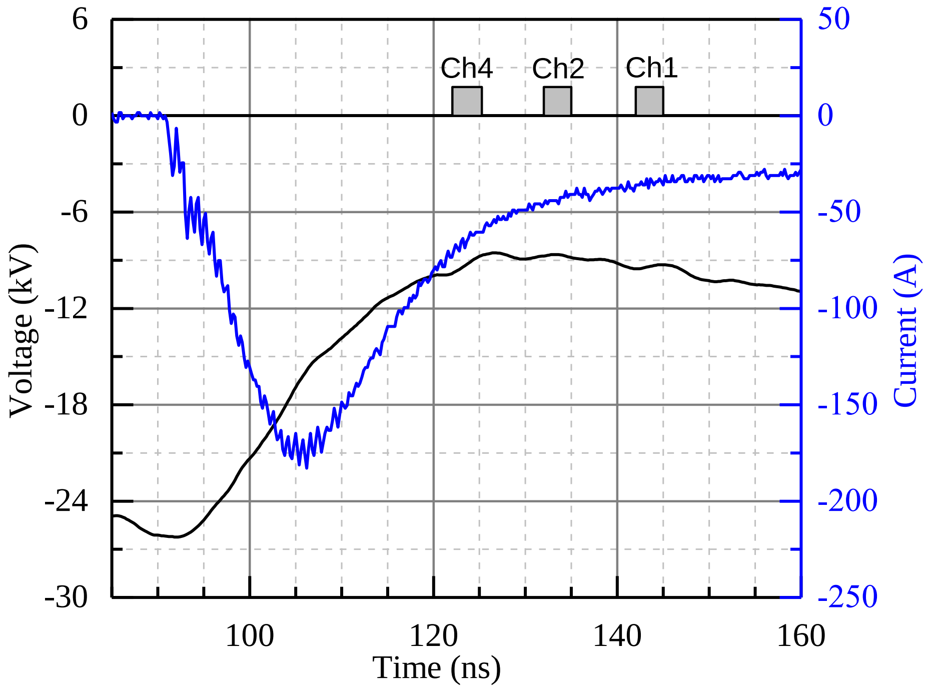

Waveforms of voltage (black) and discharge current pulses (blue). Air pressure is 100 kPa. d = 8.5 mm.

Air pressure is 100 kPa. *d* = 8.5 mm.

C4 C2 C1 C3

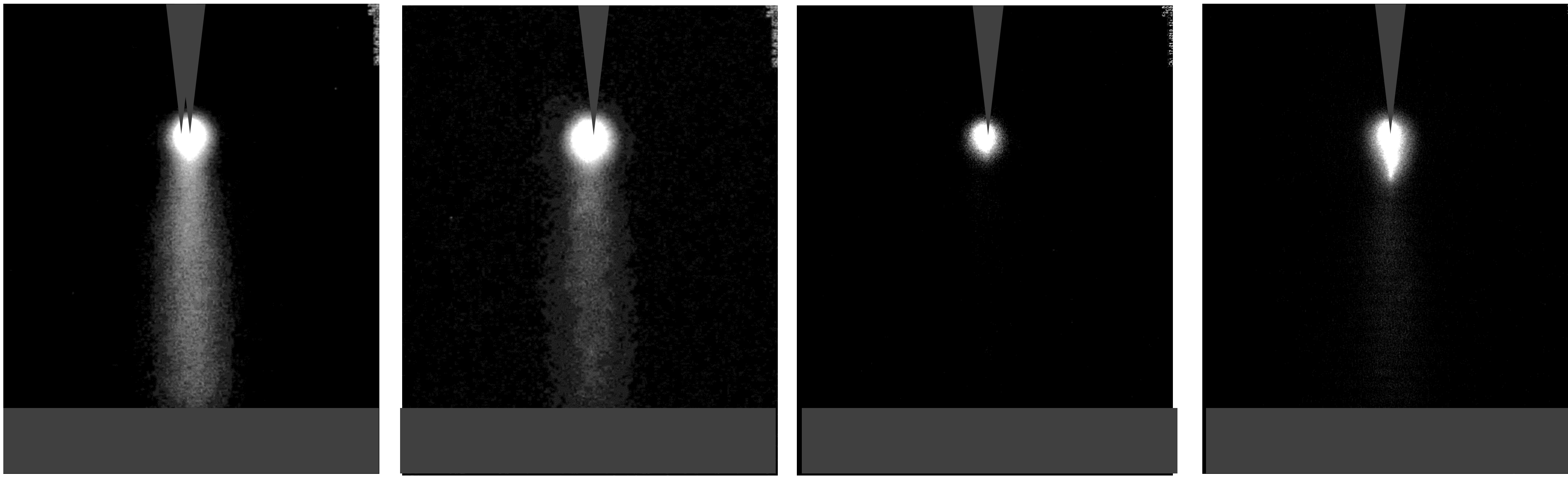

Delay = 4 ns Delay = 14 ns Delay = 24 ns Integr. 30 ns

Images of the discharge plasma glow taken with the ICCD camera.

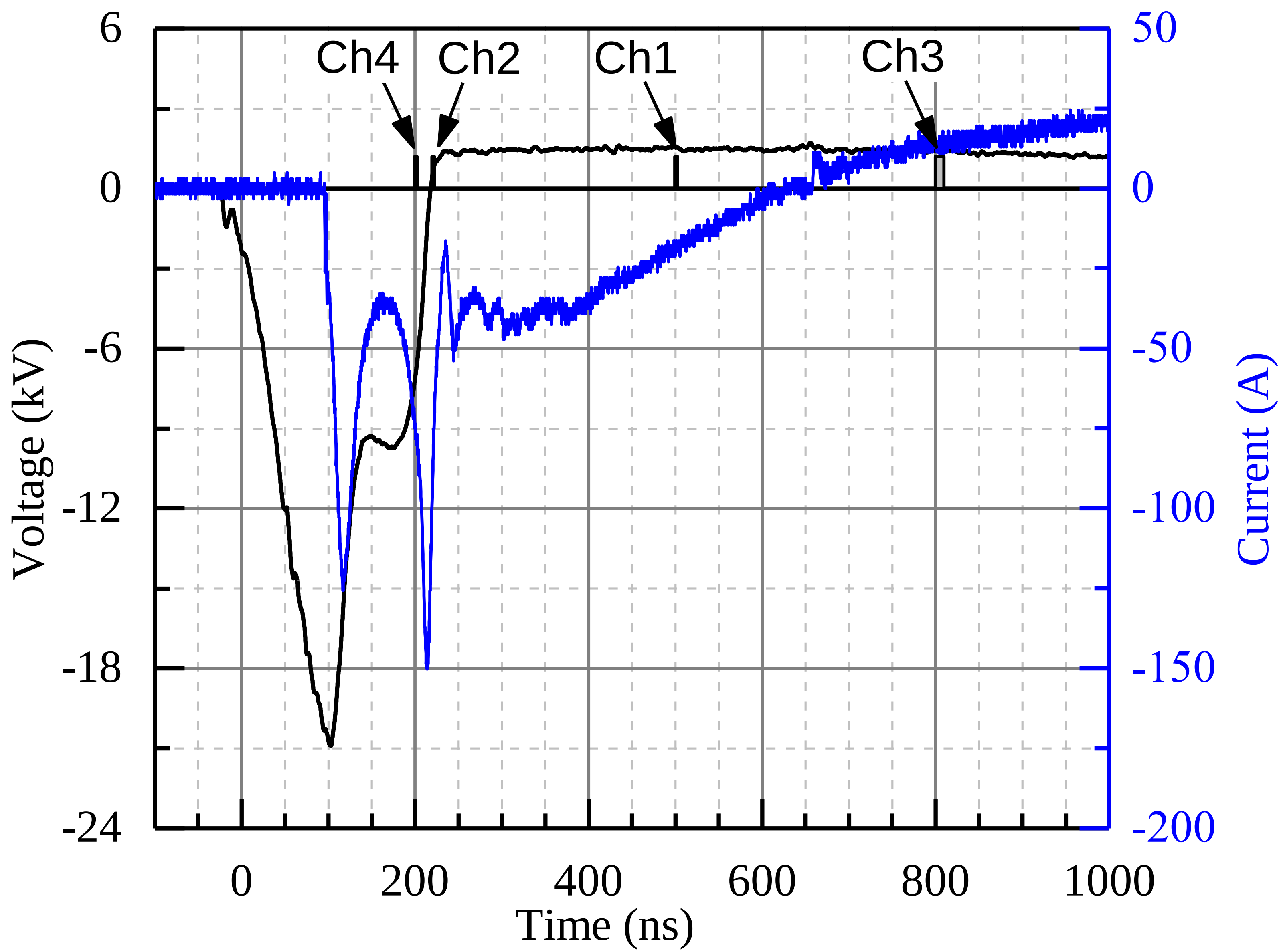

Waveforms of voltage (black) and discharge current pulses (blue).
Air pressure is 100 kPa. d = 8.5 mm.

Air pressure is 100 kPa. *d* = 8.5 mm.

C4 C2 C1 C3

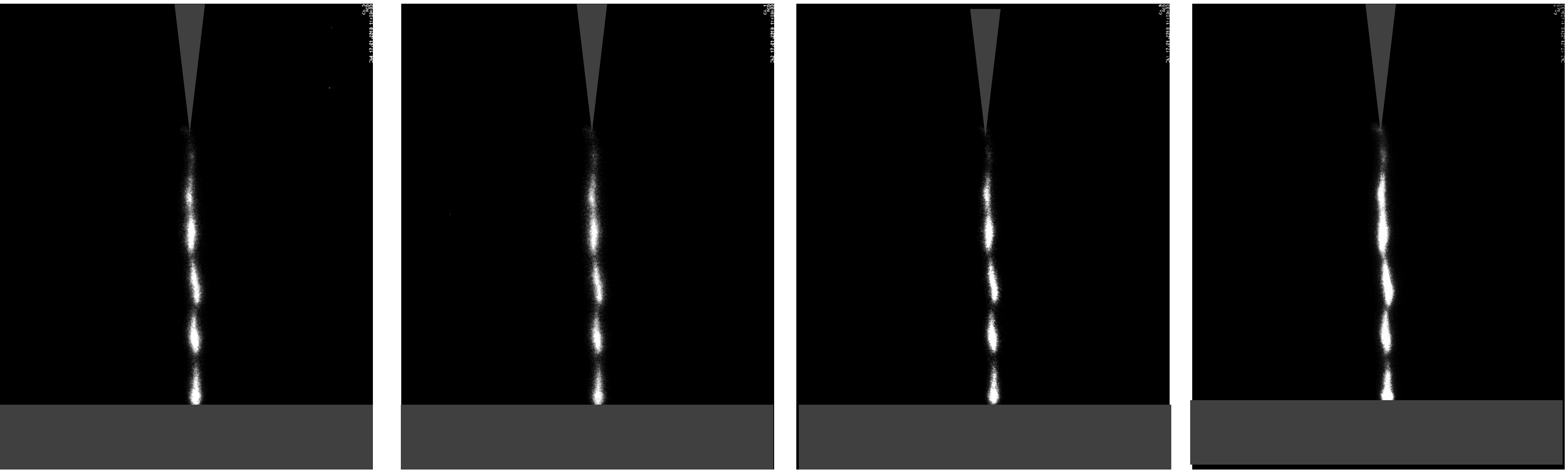

Delay = 4ns Delay = 7ns Delay = 10ns Integr. 30ns

Images of the discharge plasma glow taken with the ICCD camera.

Формирование импульсов рентгеновского излучения большой длительности за счёт тока пучка убегающих электронов при микросекундном фронте импульса напряжения

Установки с фронтом импульса напряжения 0.5 и 1.5 мкс

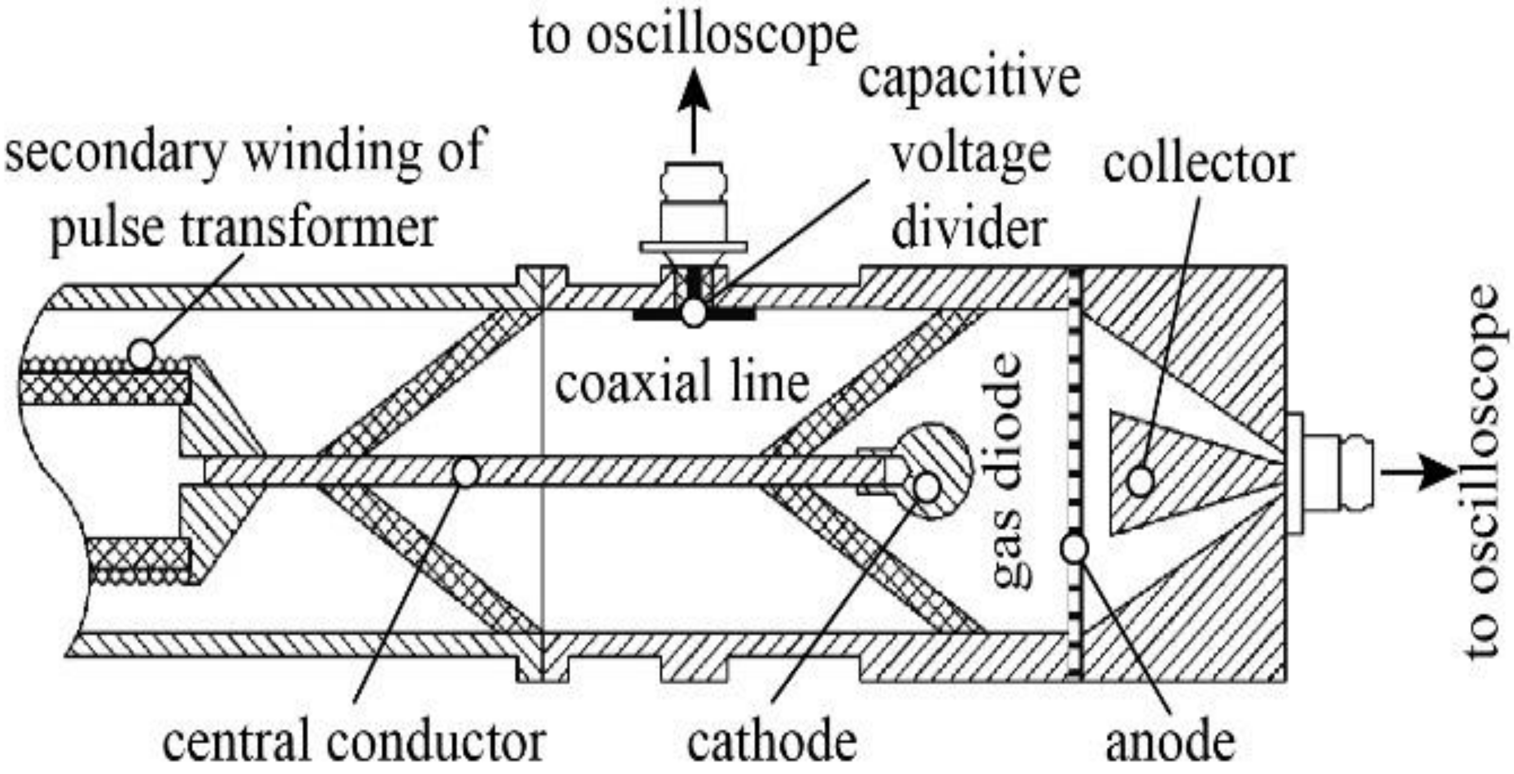

Schematic diagram of the part of the first setup including coaxial line, collector, and gas diode formed by a ball-shaped cathode and flat anode.

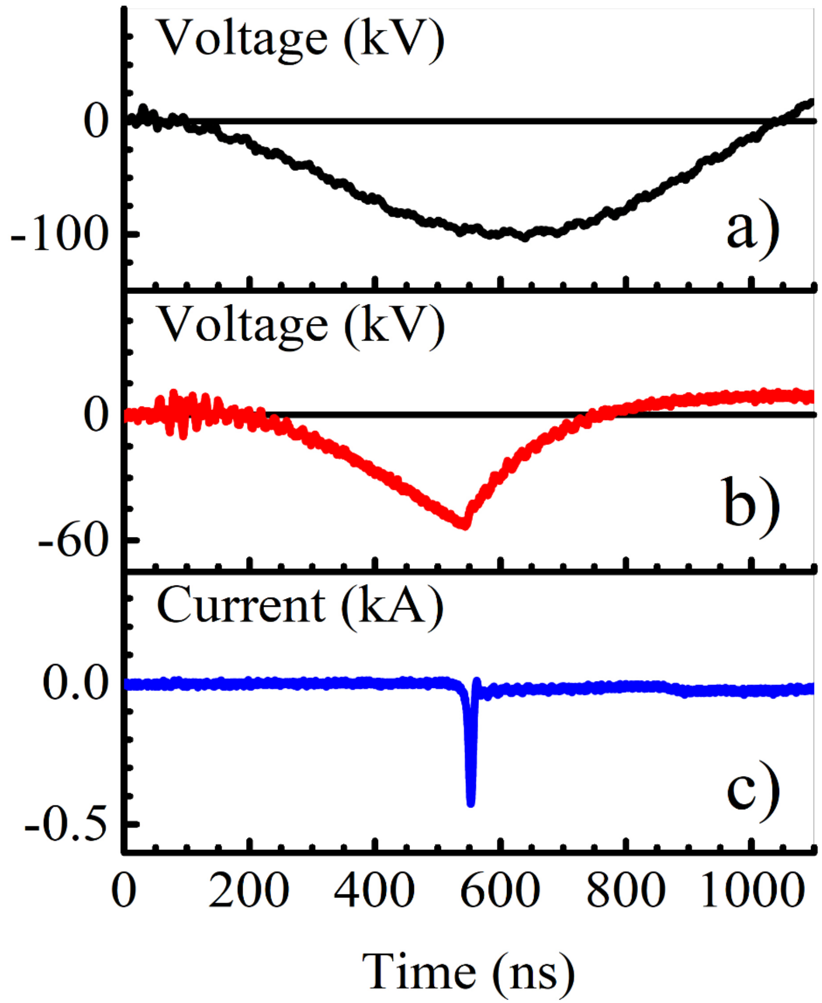

Waveforms of the voltage in idling (a), as well as of the voltage across the gap (b) and discharge current (c) when breakdown occurs. First setup.

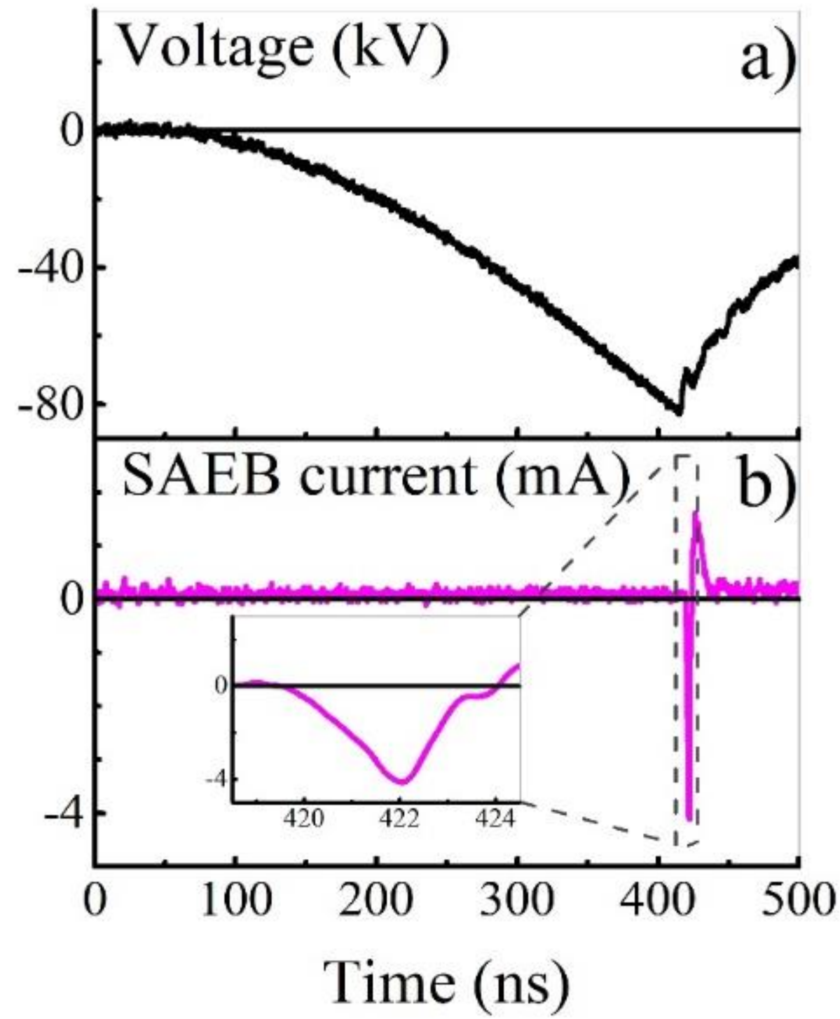

Waveforms of the voltage across the gap (*a*) and SAEB current (*b*). 15.1-mm-diameter ball-shaped cathode. The gap width is 20 mm. First setup.

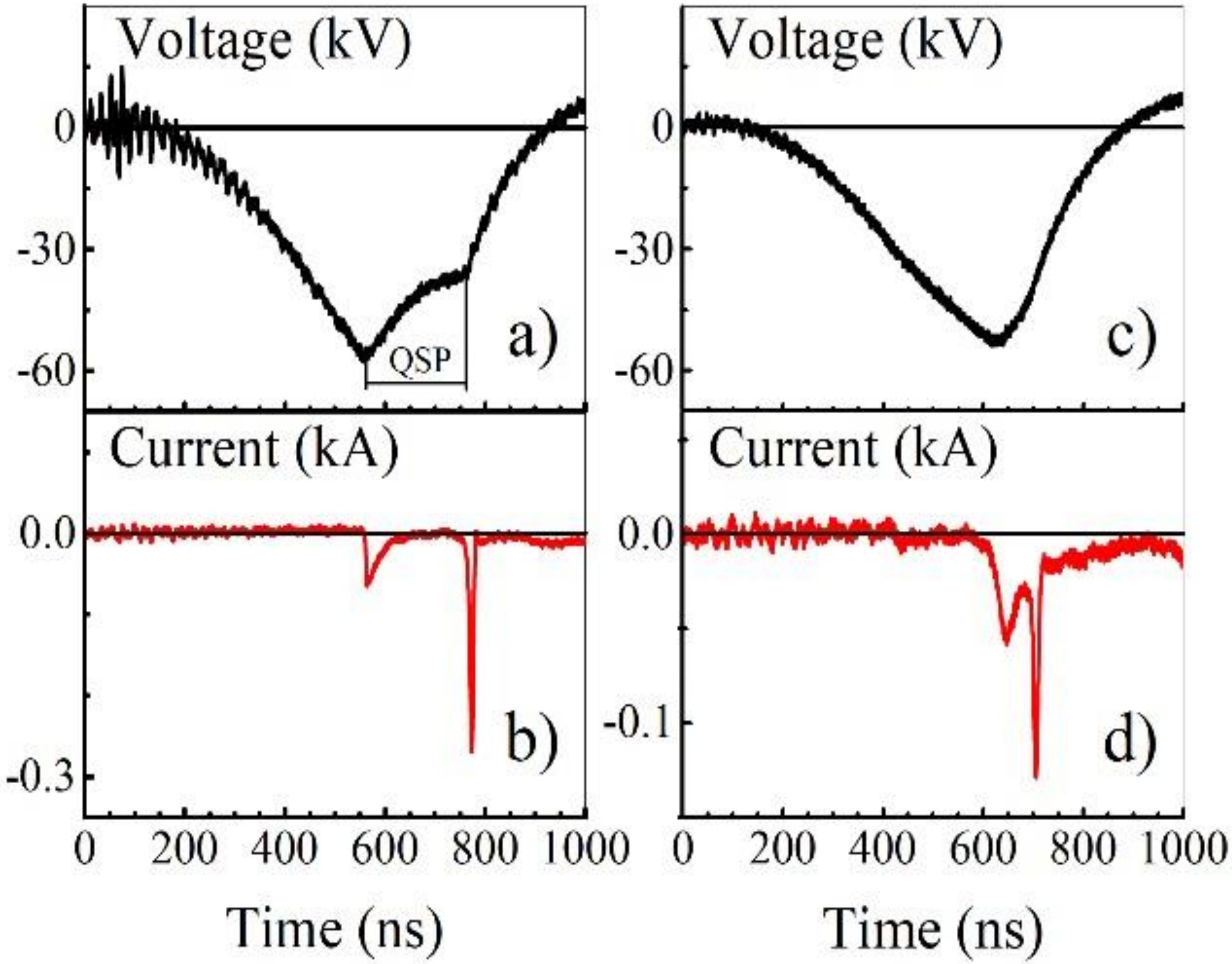

Waveforms of the voltage across the gap (a, c) and current through the gap (b, d). Cathode – stainless steel hemisphere with the radius of 17.5 mm. The gap width is 20 mm. First setup.

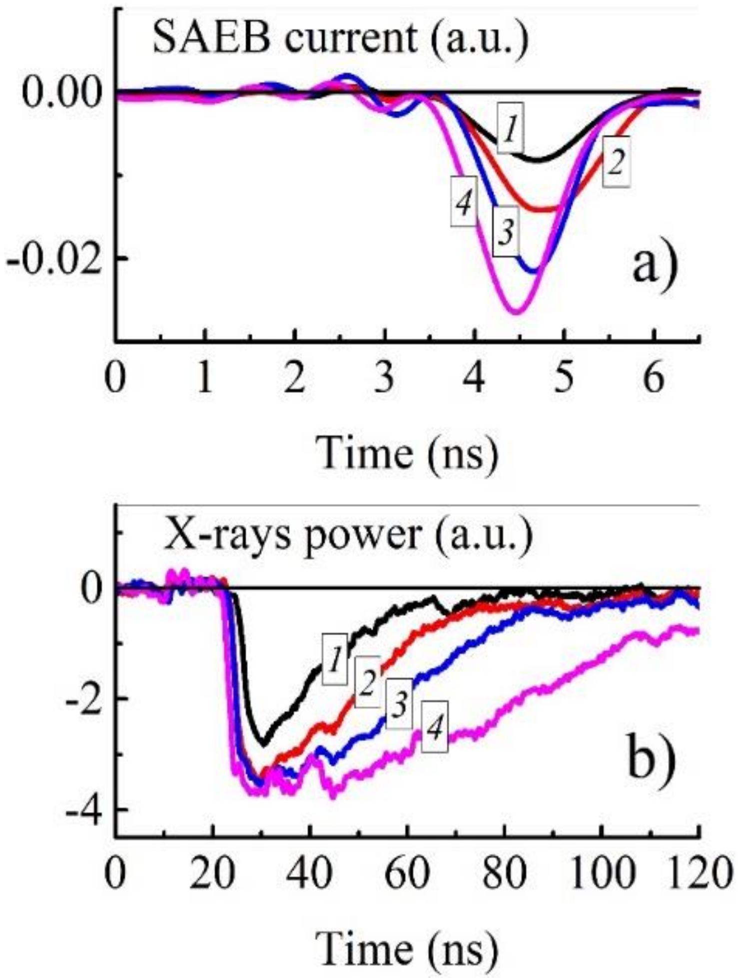

Waveforms of the RAEB current behind the anode made of kimfol film (*a*) and X-ray radiation with a 30-µm-thickness Al anode foil (*b*). 15.1-mm-diameter ball-shaped cathode. The gap width is 22 mm.
First setup.

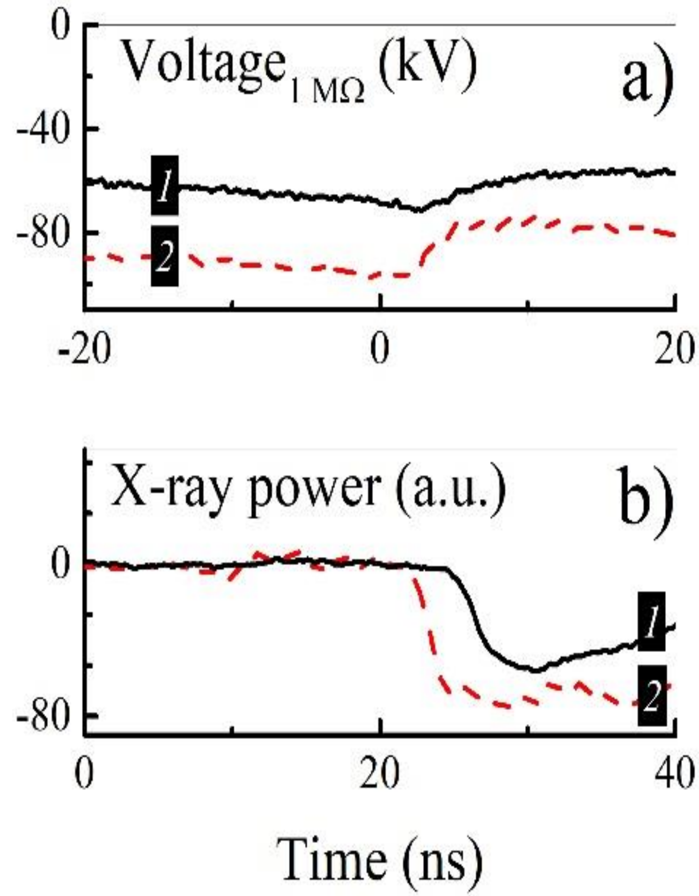

Waveforms of the voltage (a) and corresponding their waveforms of the luminescence from the scintillator exposed by X-rays (b).
First setup.

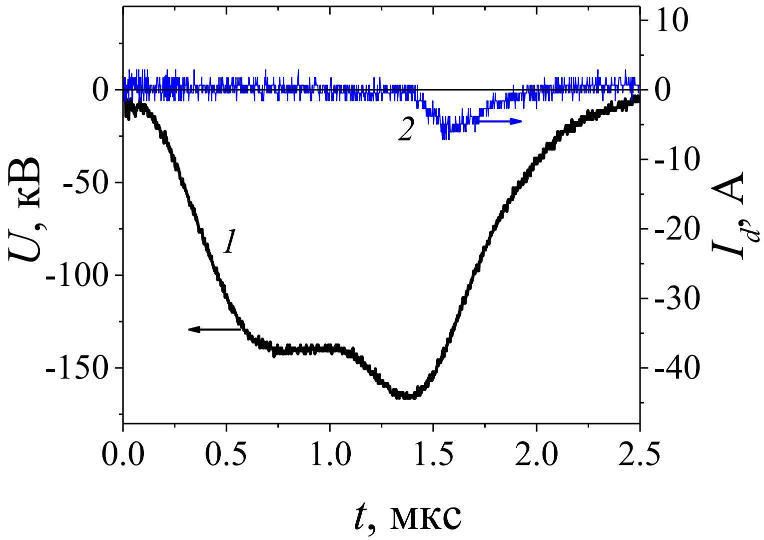

Осциллограммы импульса напряжения (1) и тока разряда (2) при диффузном разряде в воздухе атмосферного давления.

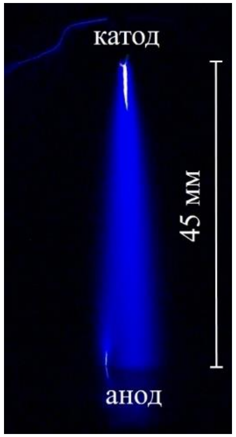

Фотография свечения диффузного разряда в воздухе атмосферного давления.

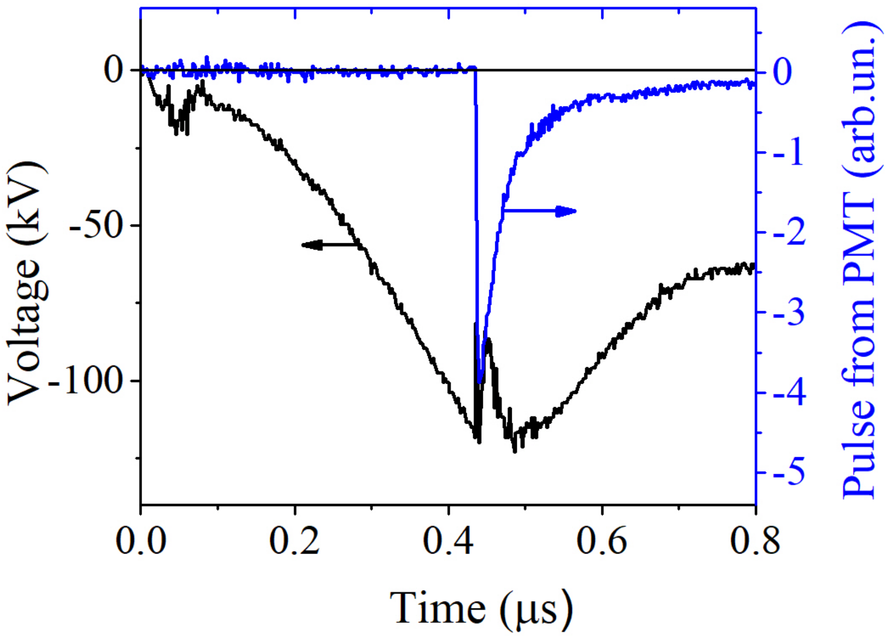

Осциллограммы импульса напряжения и рентгеновского излучения в азоте атмосферного давления .

Генерация двух импульсов тока пучка убегающих электронов

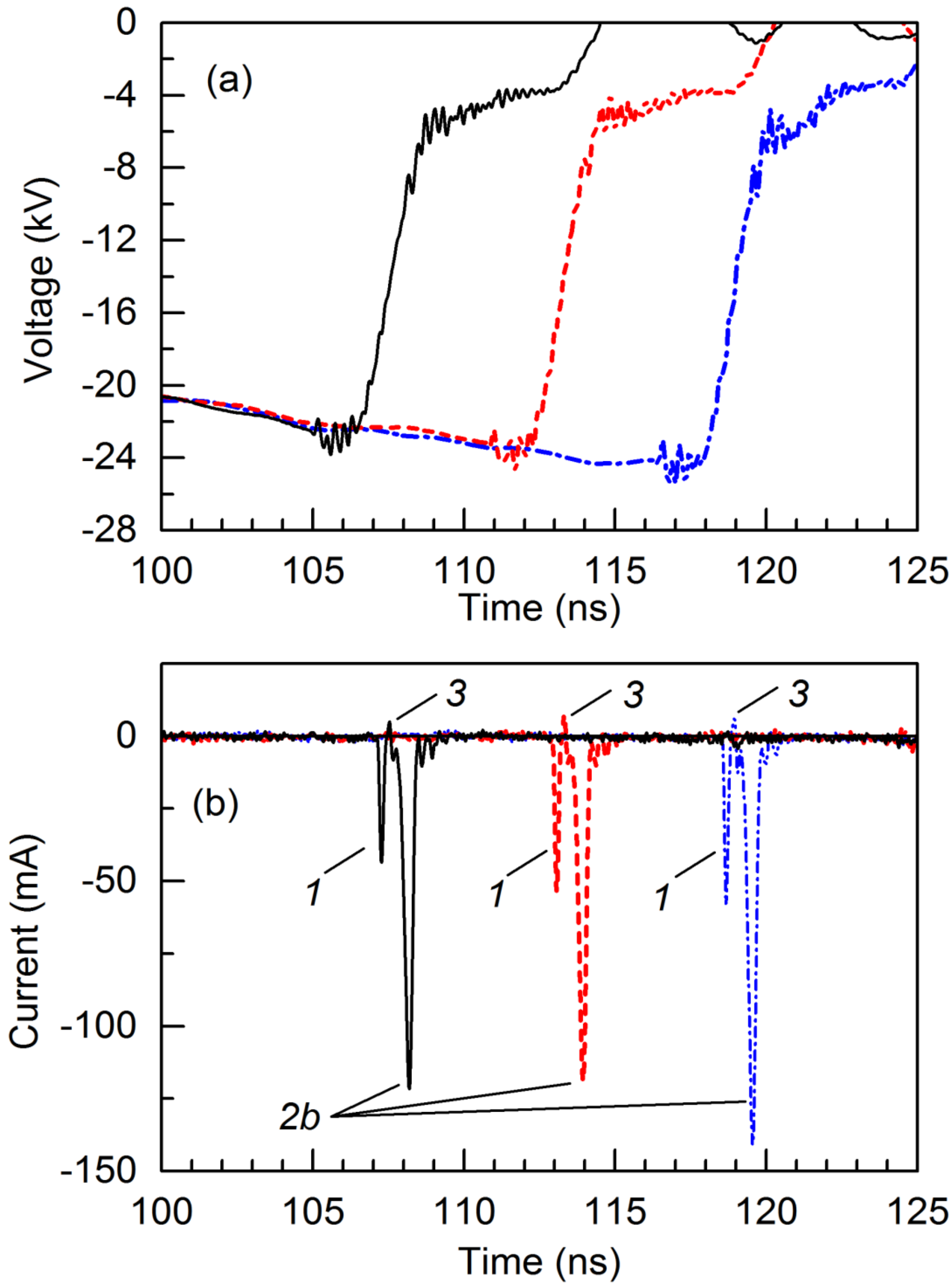

Waveforms of the (a) voltage and (b) collector current for three-discharge implementation in air at a pressure of 12.5 kPa. Anode was made of two grids. *1* – SAEB, *2b* – second beam of fast electrons. *3* – DDC when the streamer has bridged the gap.

Tarasenko, V., Beloplotov, D., Lomaev, M., & Sorokin, D. (2019). E-beam generation in discharges initiated by voltage pulses with a rise time of 200 ns at an air pressure of 12.5–100 kPa. *Plasma Science and Technology*, *21*(4), 044007.

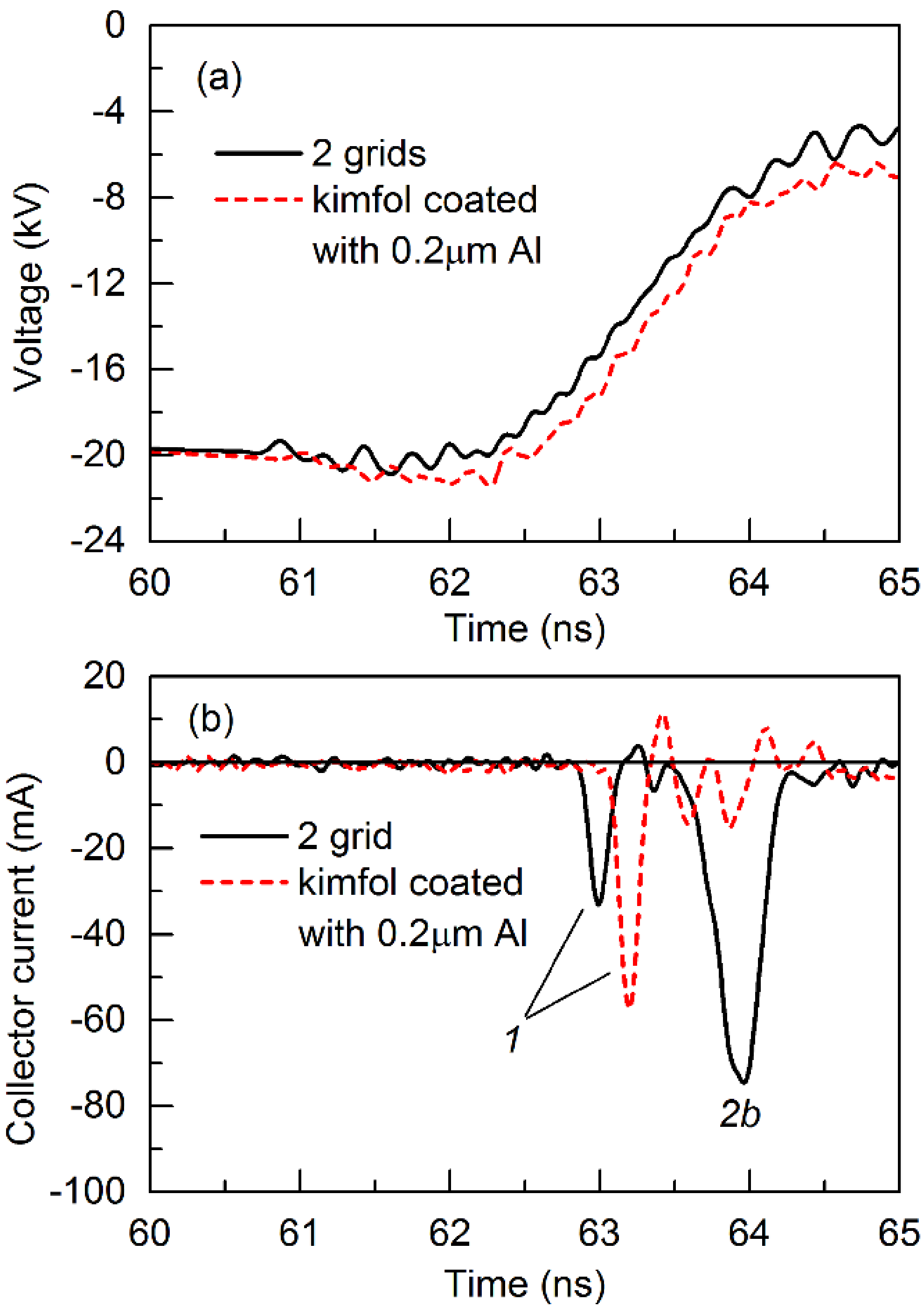

Waveforms of (a) the voltage and (b) the collector current when using anodes made of two grids and a 2 μm kimfol ($C_{16}H_{14}O_3$) film with a 0.2 μm aluminum coating at the air pressure of 12.5 kPa. Waveforms close in the breakdown delay time were chosen.

1—SAEB,

2b—second beam of fast electrons.

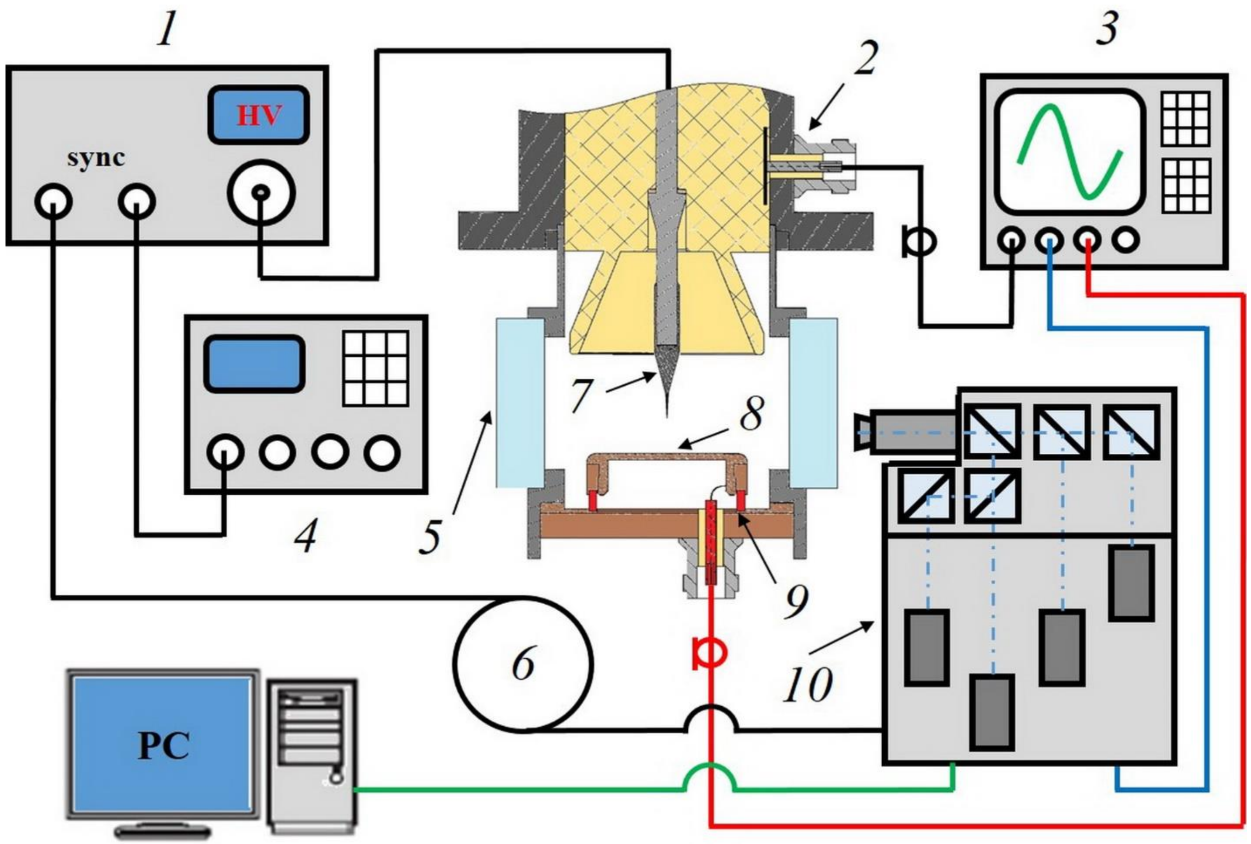

(a)

(a) Block diagram of the experimental setup for studying the streamer formation with an ICCD camera: 1 – GIN-50-1 high-voltage nanosecond generator, 2 – capacitive voltage divider, 3 – Tektronix TDS3054B digital oscilloscope (500 MHz, 5 GSa/s), 4 – trigger generator, 5 – quartz window, 6 – delay line, 7 –high-voltage electrode (a sewing needle), 8 – grounded plane electrode, 9 – current shunt made of chip resistors, 10 – HSFC–PRO four channel ICCD camera or streak camera.

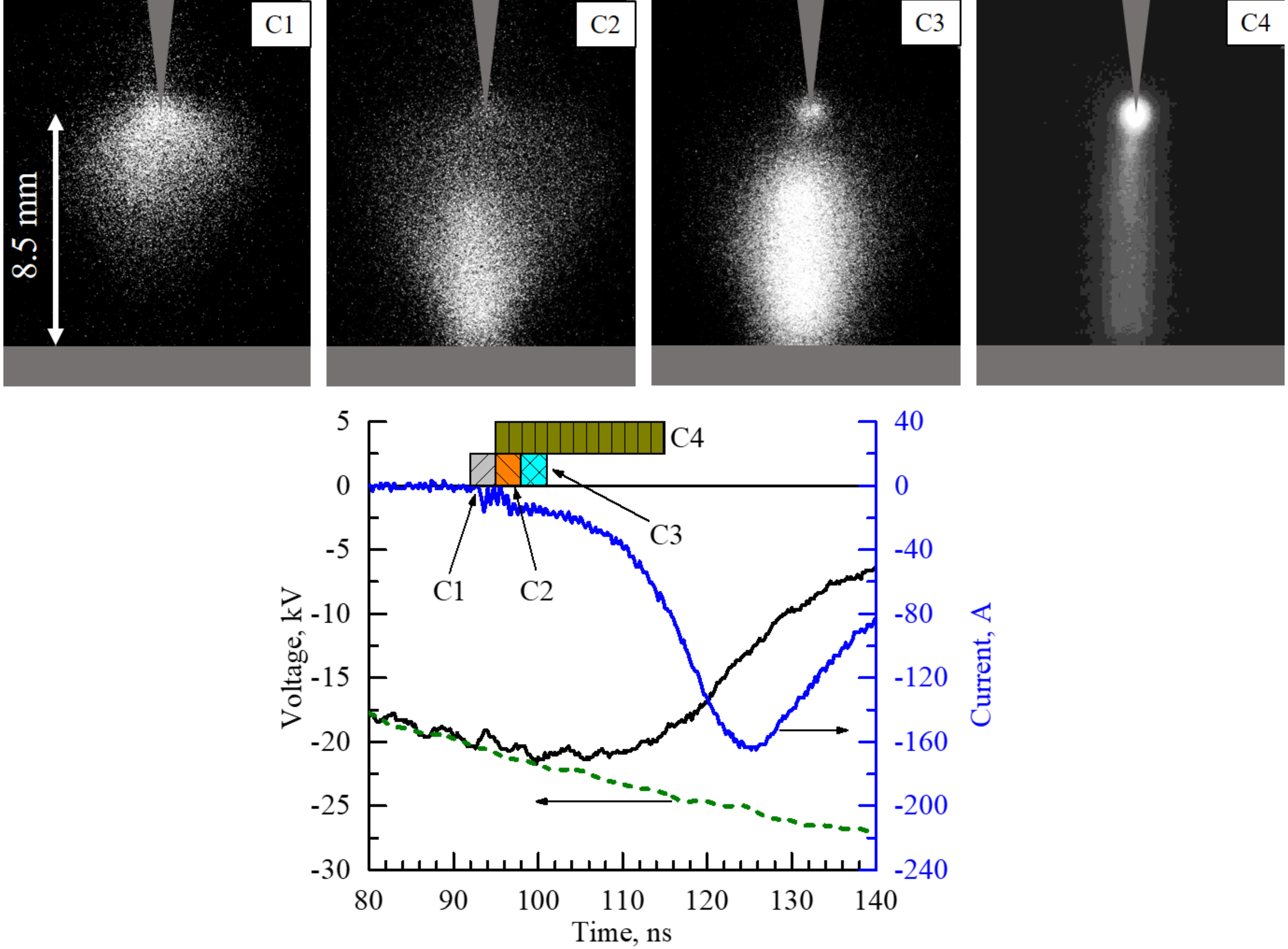

Images showing the formation of a discharge in nitrogen at a pressure of 100 kPa, obtained with a four-channel ICCD camera in one pulse, as well as the corresponding oscillograms of voltage and current. The length of the rectangles corresponds to the exposure time of each ICCD camera channel (C1 – C4). Generator number 3. The dotted line shows the open circuit voltage.

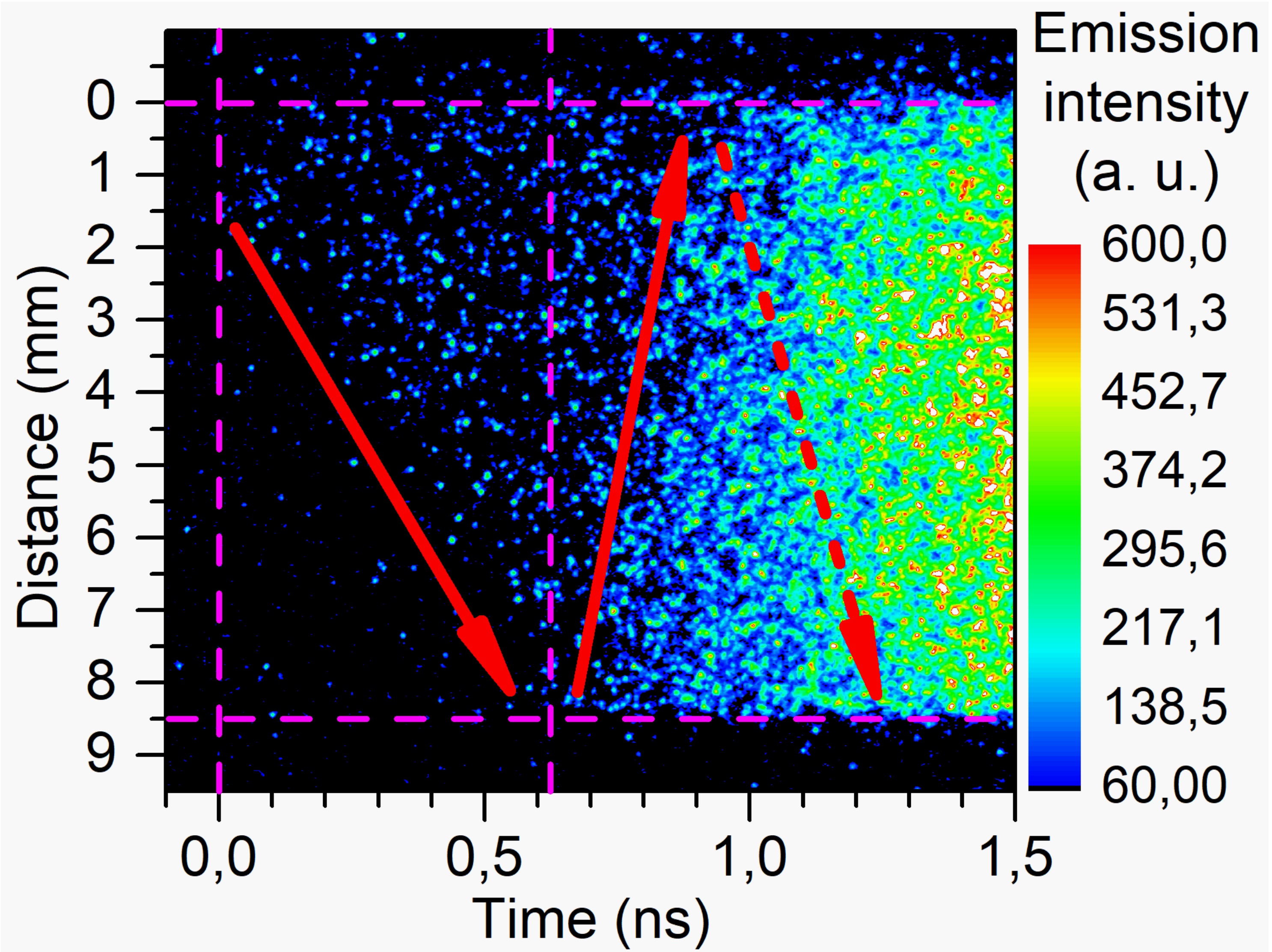

Image showing the dynamics of the plasma glow during the formation of a discharge in the gap between the tip (top) and the plane (bottom), filled with air at a pressure of 50 kPa. Generator # 2. The arrows show the direction of motion of the ionization waves.

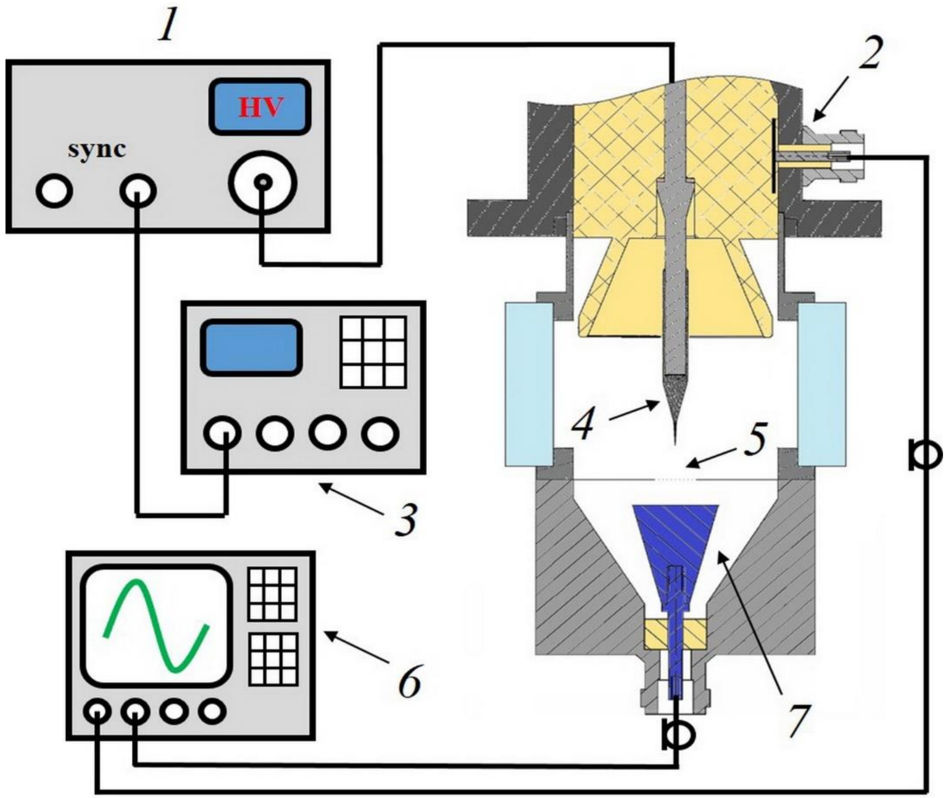

(b)

(b) Block diagram of the experimental setup for detecting runaway electron beams and dynamic displacement current caused by the redistribution of electric field strength during the streamer formation: 1 – GIN-50-1 high-voltage nanosecond generator, 2 – capacitive voltage divider, 3 – trigger generator, 4 – high-voltage electrode (a sewing needle), 5 – grounded plane electrode with 10-mm hole in the center covered by a grid, 6 – KeySight MSOS804A digital oscilloscope (8.4 GHz, 20 GSa/s), 7 – collector working in this experiment as a differential voltage divider.

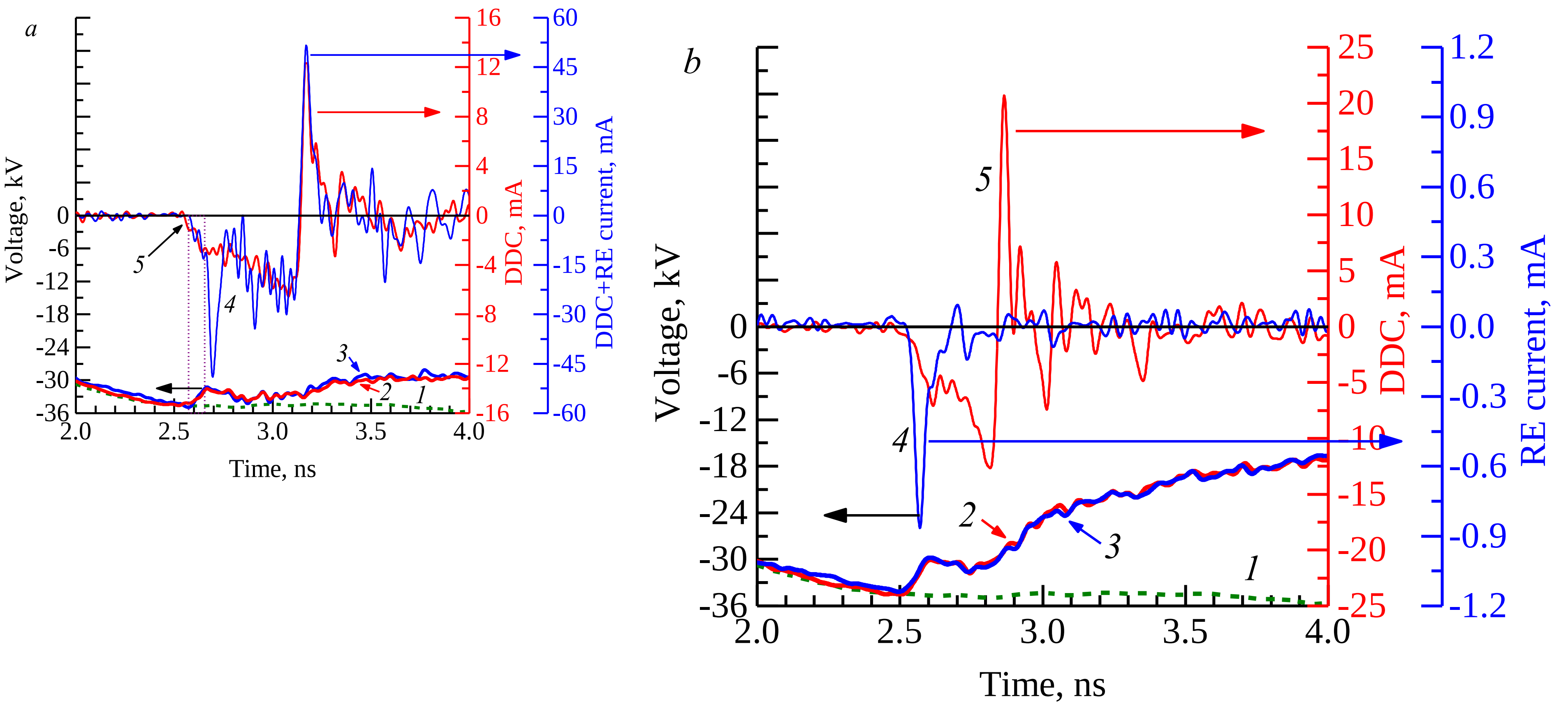

Oscillograms of the voltage in the open mode (1) and during discharge (2, 3), as well as oscillograms of the runaway electron current (4) measured by the collector, and the dynamic bias current (5), also measured by the collector. The voltage oscillogram (2) was obtained in the experiment on measuring the dynamic bias current, and the voltage oscillogram (3) was obtained in the experiment on measuring the runaway current. Air at pressure: 100 (a), 50 (b) kPa. Curve (4) at an air pressure of 100 kPa (a) was obtained by simultaneously measuring the runaway electron current and dynamic displacement current. Generator No. 2, needle-plane gap, d = 8.5 mm.

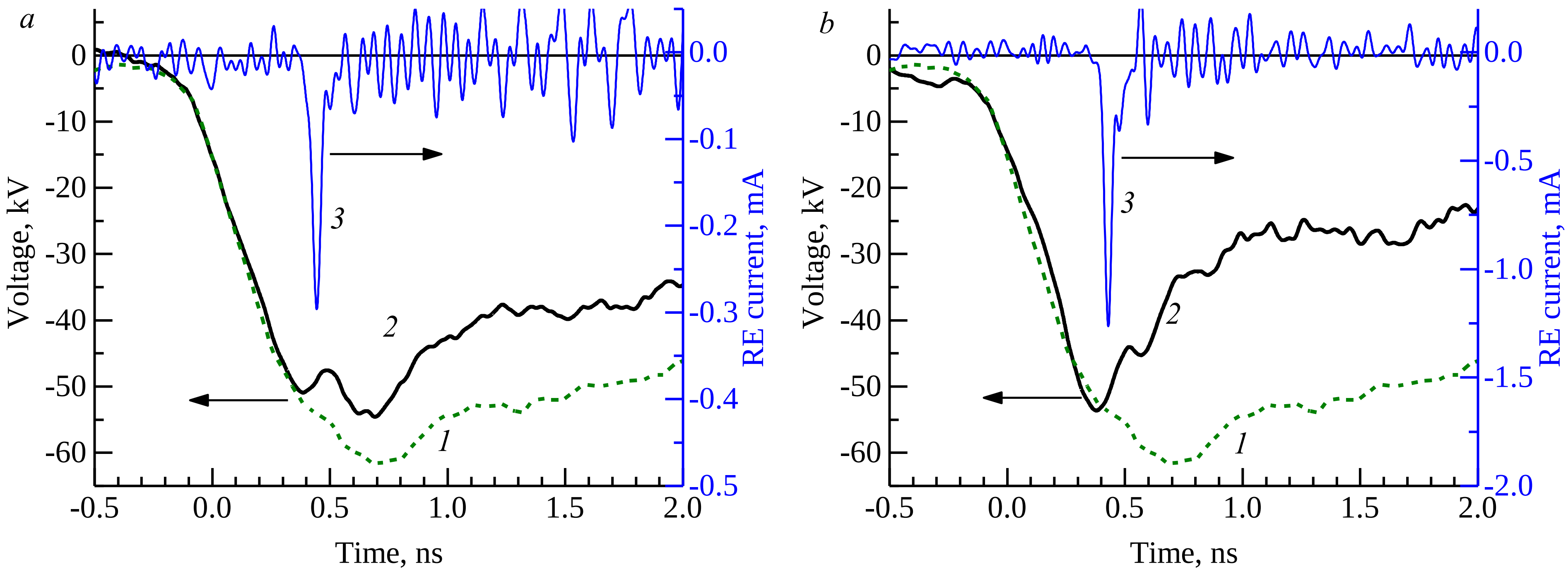

Oscillograms of the voltage in the open mode (1) and during discharge (2), as well as oscillograms of the runaway electron current. Nitrogen at a pressure of 100 (a) and 50 (b) kPa. Generator # 1, needle-plane gap, d = 8.5 mm.

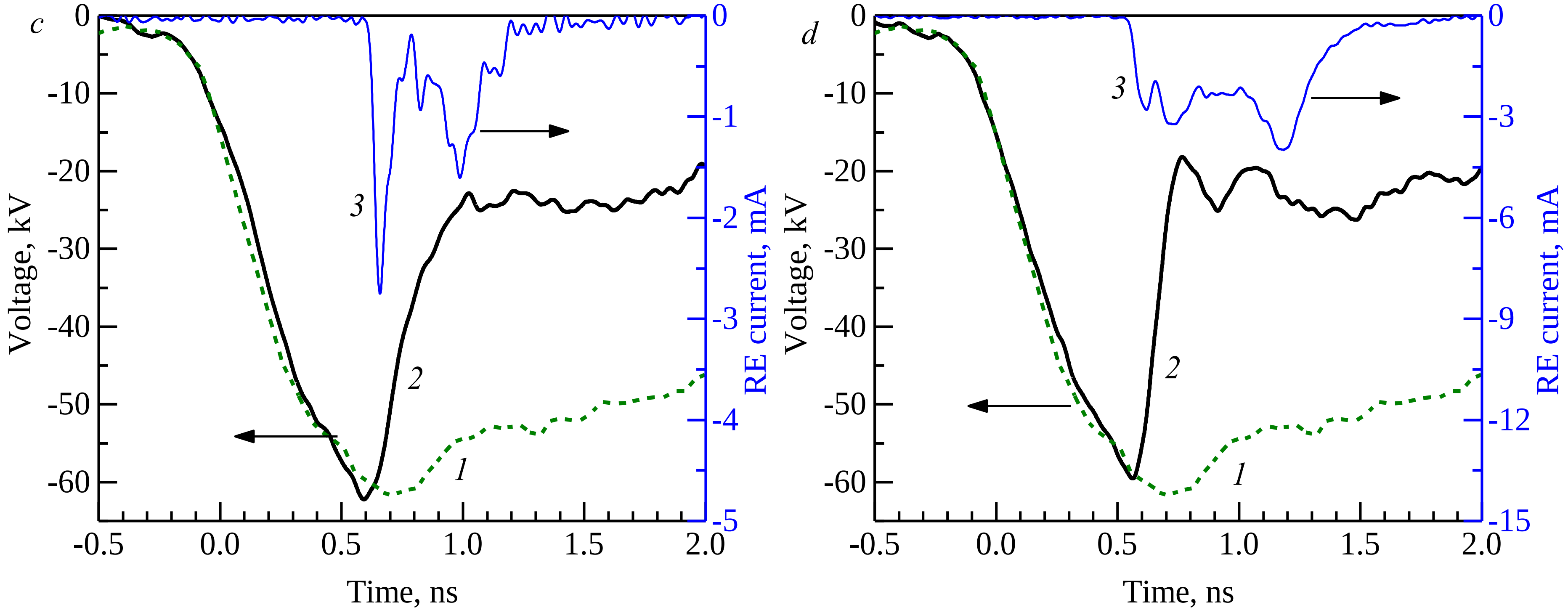

Oscillograms of the voltage in the open mode (1) and during discharge (2), as well as oscillograms of the runaway electron current. Nitrogen at a pressure of 25 (c) and 12 (d) kPa. Generator # 1, needle-plane gap, d = 8.5 mm.

Formation of two current pulses of the runaway electron beam.

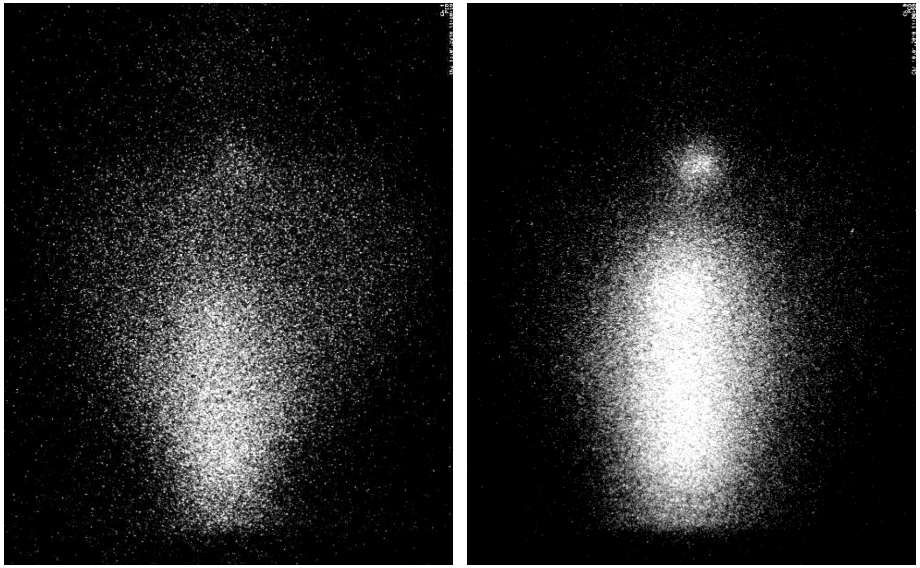

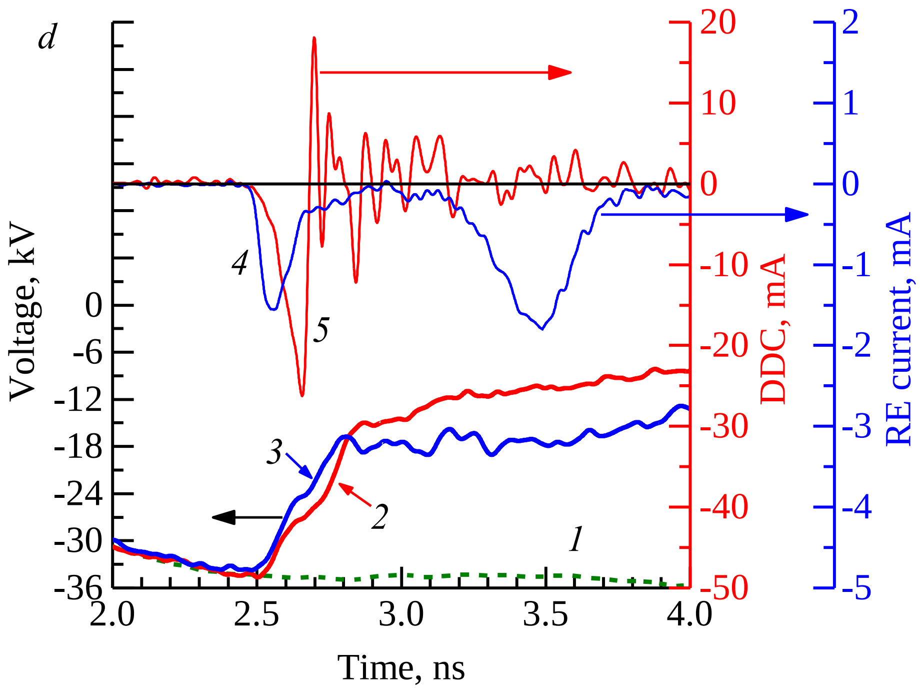

To generate the second pulses of the beam current, which are recorded after the passage of the first ionization wave and a decrease in the voltage across the gap, additional amplification of the electric field is required. This is achieved at low average E / p in two regions, due to the accumulation of positive ions at the cathode and due to an increase in the electric field at the front of the second ionization wave, which starts from the anode. The second ionization wave has a high conductivity, which follows from the intensity of its luminescence, and provides a partial removal of the anode potential to the cathode region. The factor limiting the generation of the second pulse of the beam current under these conditions is the explosive emission of electrons, which leads to a decrease in the electric field strength in the cathode layer.

Formation of the continues beam current after the first pulse without a pause.

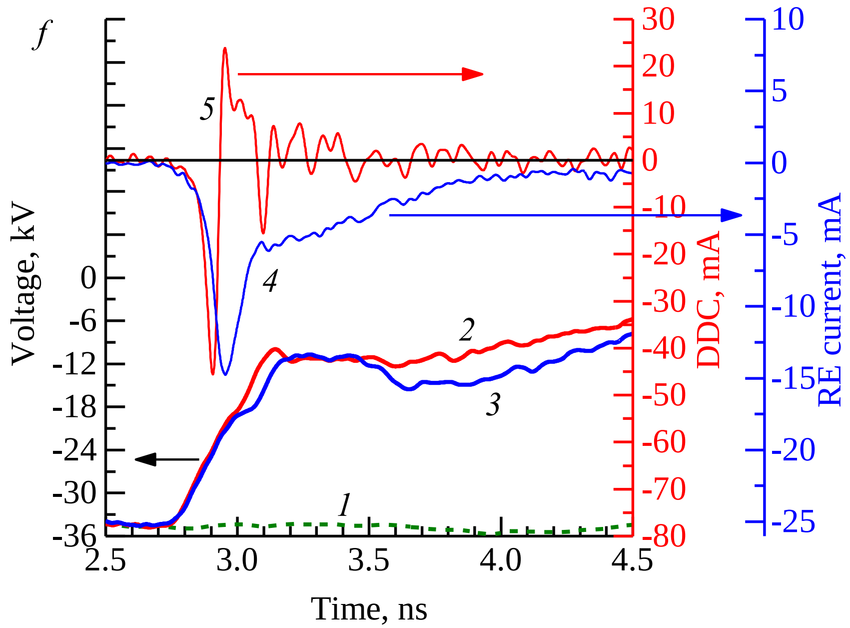

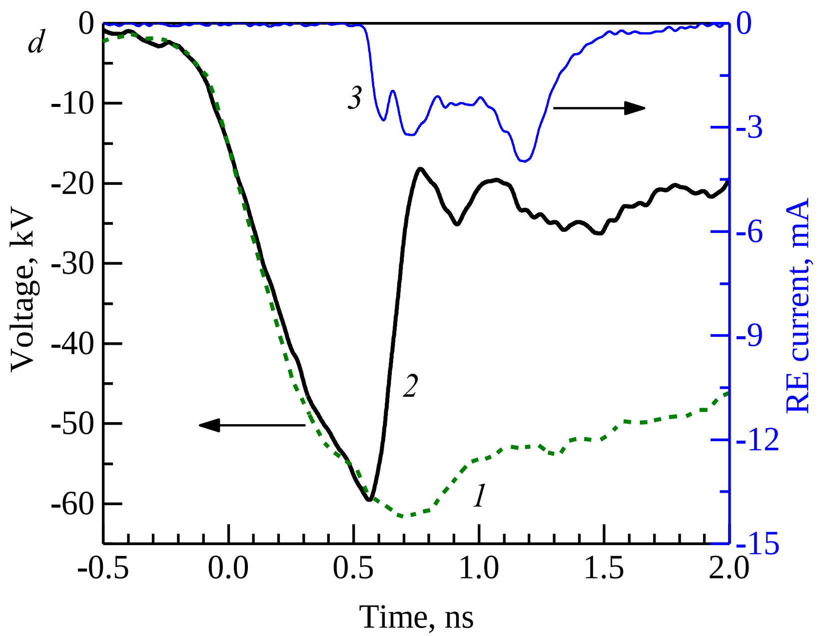

The beam current generation mode, which is transient to the conditions of a vacuum diode, is realized at relatively high average E / p due to a significant decrease in the gas pressure (3 and 12 kPa). In this mode, after the first pulse of the beam current, a quasi-stationary electron beam with a duration of 1 ns is recorded without a pause, the amplitude of which increases with the reduction of the leading edge of the voltage pulse.

Научный совет РАН по физике низкотемпературной плазмы
24 декабря 2020 г.

Выводы

Генерация убегающих электронов в газах высокого давления является фундаментальным физическим процессом и, в частности, обеспечивает формирование диффузных разрядов.

Режимы генерации пучков убегающих электронов весьма разнообразны и зависят от параметров импульса напряжения, сорта и давления газа, а также от конструкции газового диода и катода.

Thanks for your attention

Edited Collections [2014 E, 2015 R, 2016 (V.1 and V.2)E and books 2020 R]

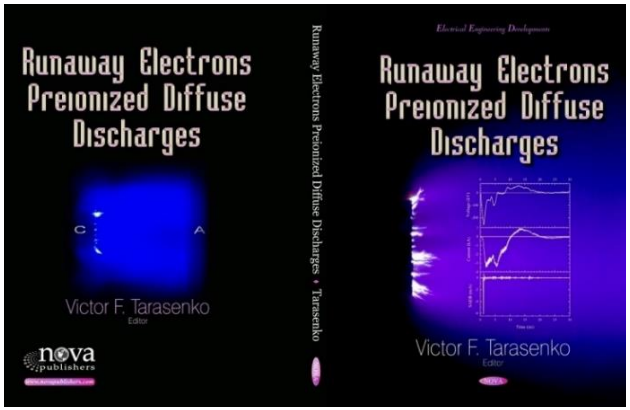

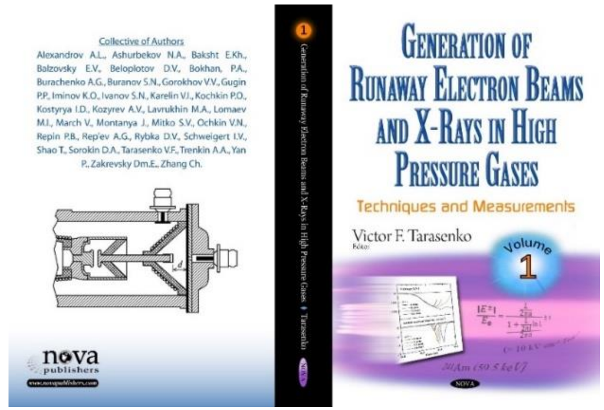

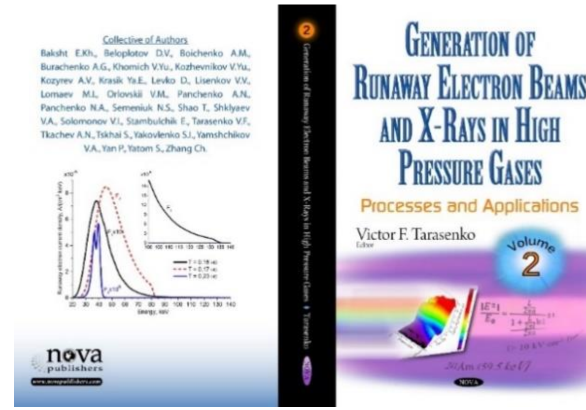

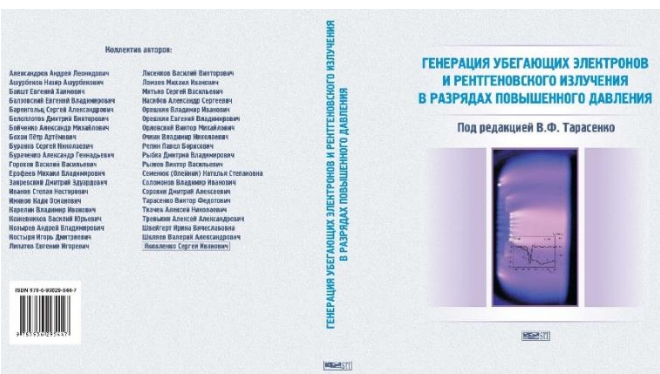

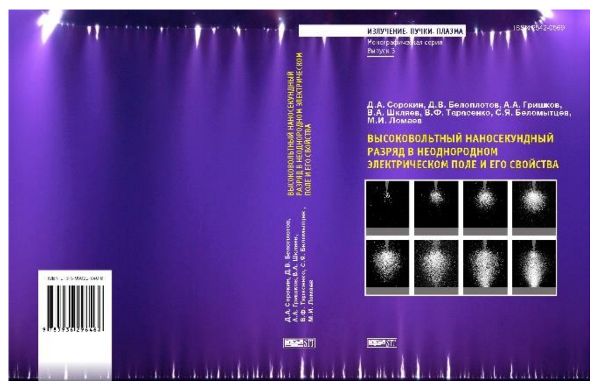

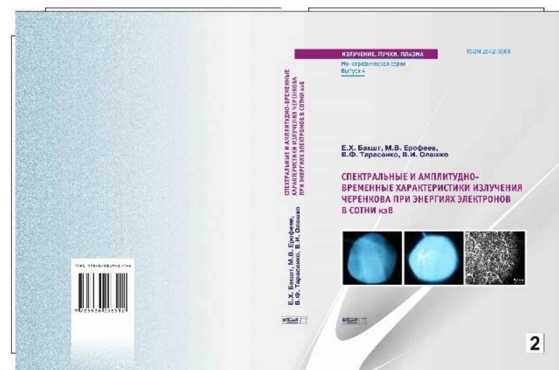

Наши коллективные монографии и монографии